Stony Brook University

Topical Treatment of Actinic Keratosis and Non-melanoma Skin Cancer with Phospho-sulindac and Difluoromethylornithine

A Thesis Presented

by

Yajing Sun

to

The Graduate School

in Partial Fulfillment of the

Requirements

for the Degree of

Master of Science

in

Chemistry

Stony Brook University

May 2015

Stony Brook University

The Graduate School

Yajing Sun

We, the thesis committee for the above candidate for the

Master of Science degree, hereby recommend

acceptance of this thesis.

Basil Rigas – Thesis Advisor
Departments of Medicine and of Pharmacology

Peter Tonge – Second Reader
Professor, Department of Chemistry

Jonathan Rudick –Third Reader
Assistant Professor, Department of Chemistry

This thesis is accepted by the Graduate School

Charles Taber
Dean of the Graduate School

Abstract of the Thesis

Topical treatment of Actinic Keratosis and Non-melanoma Skin Cancer with Phospho-sulindac and Difluoromethylornithine

by

Yajing Sun

Master of Science

in

Chemistry

Stony Brook University

2015

Actinic keratosis (AK), a cutaneous lesion resulting from the proliferation of atypical epidermal keratinocytes, has an incidence of 11%-26% and its prevalence is 58 million in the US alone. AK is a precursor to non-melanoma skin cancer (NMSC). NMSC, consisting of squamous cell and basal cell carcinomas, represents the most frequent human cancer. Current treatment for AK and NMSC is often limited by low efficacy, side effects, high cost, and undesirable cosmetic outcomes. Thus new agents for the treatment of AK are urgently needed.

In an effort to develop an efficacious, safe and patient-acceptable approach to both AK and NMSC, we developed a topically applicable drug combination consisting of the novel agent phospho-sulindac, a modified non-steroidal anti-inflammatory drug, and difluoromethylornithine an inhibitor of polyamine synthesis. The two agents were formulated in a pluronic lecithin organogel. After

a systematic evaluation of penetration enhancers using *in vitro* dermal drug diffusion and *in vivo* pharmacokinetic studies, we developed an optimal formulation which we evaluated *in vivo*.

For NMSC we used an intradermal A431 human skin cancer xenograft in nude mice that provides a therapeutic model for the topical application of test agents. For AK, we used the UV irradiation model that recapitulates many aspects of the injurious effect of solar radiation on the skin, the main cause of AK.

The topical application of phospho-sulindac and difluoromethylornithine combination reduced NMSC by 71%. The effect was mediated in part through suppression of intracellular polyamine levels; polyamines control cell proliferation.

The PS/DFMO topical application had remarkably strong effect on AK. PS/DFMO induced lesion regression evident in a few days (tumor volume 51% on day 7). By the end of the study (day 22), compared to time 0 values, the lesion volume/mouse was 62% lower and the lesion number/mouse was 70% lower. Importantly, 51% of the animals were lesion-free. *Efficacy comparison* to the widely used diclofenac gel 3% showed that after 15-days of treatment, diclofenac had no efficacy at all but significant side effects. No animal on PS/DFMO had any *side effects*, topical or systemic, from PS/DFMO. Mechanistically, PS/DFMO acts at least in part though polyamines and the cellular redox status. PS/DFMO reduced significantly polyamines in AK skin. Compared to normal mice never exposed to UV, AK mice had markedly elevated levels of urinary 15-Isoprostane F_{2t}, a marker of oxidative stress. PS/DFMO eliminated the oxidative stress associated with AK.

PS/DFMO is a promising topical drug combination of the treatment of NMSC and AK.

Table of Contents

Chapter One
Skin Neoplasias and the Development of Novel Treatments

Chapter Two
Development of a Topical Treatment for NMSC and AK

Chapter Three

Efficacy Studies

Part I: A431 skin xenograft study

List of Figures

List of Tables

List of Abbreviations

8-OHdG	8-hydroxy-2' -deoxyguanosine
AUC	area under the concentration-time curve
COX	cyclo-oxygenase
DAB	3,3'-Diaminobenzidine
dd water	distilled deionized water
DFMO	L-α-difluoromethylornithine
NSAID	non-steroidal anti-inflammatory drug
PBS	phosphate-buffered saline
PCNA	proliferating cell nuclear antigen
PLO	pluronic lecithin organogel
PS	phospho-sulindac
ROS	reactive oxygen species
TUNEL	terminal deoxynucleotidyl transferase dUTP nick end labeling
UV	ultraviolet

Acknowledgments

I would like to express my gratitude to my research advisor, Dr. Basil Rigas, for providing me the opportunity to work and learn in his laboratory. He encouraged me to pursue my dreams of study in the pharmaceutical area, helped me when I faced difficulties with my research and offered extensive advice on presentation, writing, and career choices and even life, often using his short and wise stories.

Next, I would like to thank my committee members, Dr. Peter Tonge, and Dr. Jonathan Rudick for their invaluable suggestions and interest in my work. Their advice has helped me throughout this thesis and defense process, and I am grateful.

Completing my thesis work would not have been possible without the generous assistance of Dr. Manjeet Deshmukh, Dr. Georgios Matthaiolampakis Dr. Ka-Wing Cheng， Ms. Liqun Huang， Dr. Nengtai Ouyang, and Dr. Gang Xie. Because of the outstanding body of work in the field of cancer prevention that they have generated, I was able to progress much further during my studies here than I could have ever hoped. I would also like to give a special thank you to Ms. Carol Ann Amella for her editing assistance and her incredible management and organization of the lab. I would also like to thank Drs. Gerardo Mackenzie and Jennie Williams for their selfless support. A special note to thanks all of additional personnel in the Division of Cancer Prevention for creating such a friendly working environment for me.

In addition, I would like to thank my friends, especially Baisakhi Mukherjee, Lengfang Cui, and Shuo Wang. I appreciate their friendship and company when I needed support.

Finally, I would like to give a heartfelt thank you to my parents and grandparents for their love and support both moral and financial. Because of you, I can pursuit my dreams without any hesitation.

Chapter One

Skin Neoplasias and the Development of Novel Treatments

1. Actinic keratosis

Actinic keratosis (AK) is the most common type of skin disease in the Caucasian population[1]. The AK lesions commonly occur in areas of the skin easily exposed to sunlight, such as the head, the balding scalp, the face, and the back of arms and hands. The development of AK is attributed to excessive ultraviolet (UV) exposure, as for example from sunlight and treatments in tanning salons[2]. Clinically, the AK lesions appear as raised, scaly, red bumps on the skin. However, the clinical manifestations of AK are not always that clear-cut[3].

AK is characterized by proliferation of neoplastic keratinocytes limited to the epidermis, marked by architectural disorder. These features include abnormal keratinocytes of the basal layer, nuclear atypia and hyperkeratosis of the epidermis. Atypical nuclei are enlarged irregular, and hyperchromatic. 4

The major mechanisms leading to the development of AK are inflammation, oxidative stress, immunosuppression, impaired apoptosis, mutagenesis, uncontrolled cell proliferation, and issue remodeling[4]. Infection with human papilloma virus (HPV) has been reported by Alan Storey. et al as another possible cause of AK lesions[5]. AK is considered to be a potentially pre-cancerous condition[2], and without proper treatment, AK carries an increased risk of developing into squamous cell carcinoma and other skin malignancies[6]. Although most AKs do not progress to squamous cell carcinoma, AKs that do progress to squamous cell carcinoma cannot be distinguished from AKs that will spontaneously resolve or persist[7].

1.1. The underestimated incidence of AK

Even though AK is prevalent with increasing incidence, its recognition is still low. A survey by Hanson et al in 2004 showed that 90% of primary care physicians are more familiar with basal cell carcinoma than with AK[8]. Most of the primary care physicians on average referred their patients with AK to surgeon or plastic surgeons, especially in Europe[6]. Moreover, the public needs to be made more aware of the dangers associated with AK. The most common statements from the public include: “It would go away,” “It is not important”, and “It could self-treat”[9]. Even though the public realizes that sunlight is damaging to the skin, they do not have the same consideration towards tanning salons. As a result of underdiagnosis of PK by primary care physicians and the lack of awareness of the public, the prevalence of AK is increasing, and may result in an increased burden of non-melanoma skin cancer[6].

1.2. Mechanism of UV-induced AK

UV radiation is a complete carcinogen, which can induce the initial genetic mutations in keratinocytes, and promotes tumor cell expansion. Indeed, UV radiation is considered the most frequently encountered carcinogen by humans[11]. UV light is divided into three different regions based on wavelength: 94% to 97% is UVA (320-400 nm wavelength), 3% to 6% is UVB (290-320 nm wavelength), and a minimal amount is UVC (200-290 nm wavelength)[10].

UV radiation generates disorder to cell growth and differentiation, inflammation, and immunosuppression through pathways including DNA photodamage, changes in membrane phospholipids, and reactive oxygen species (ROS). When the skin receives continually excessive UV exposure, damage occurs, and skin cells may suffer abnormal apoptosis and aberrant proliferation.

The final result is the development of AK. [4] Fig.2 summarizes this mechanism by which UV radiation causes AK.

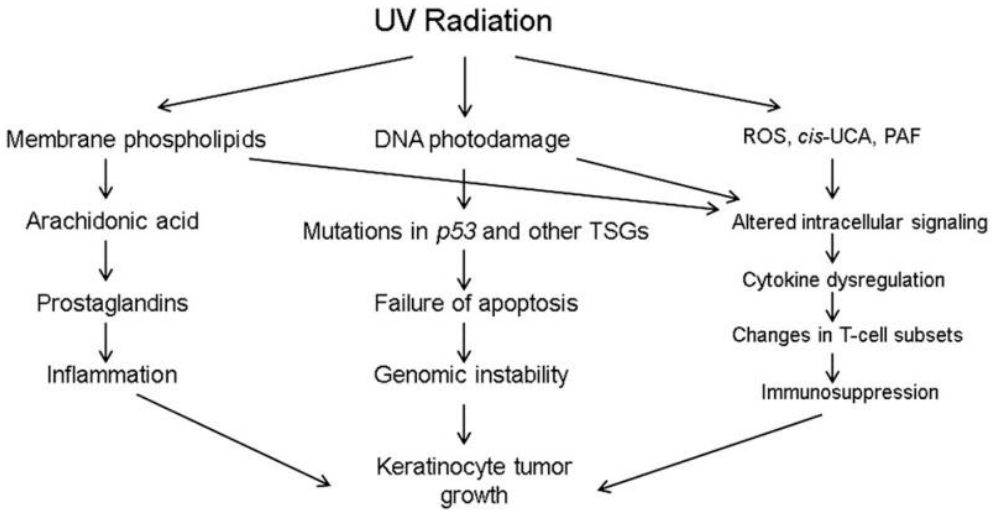

Figure 1. Mechanism by which UV radiation causes AK (ref.11)

Genetic mutations

Expression and activation of p53 in the epidermis protects from UV-induced skin disorders. However, continual UV exposure (especially UVB) may induce genetic mutations. The signature mutations of UVA are thymine (T) →guanine (G), due to the formation of 8-hydroxyguanine adducts. UVB (290-320 nm) irradiation directly causes the formation of cyclobutane pyrimidine dimers and 6-4 photoproducts, which in turn give rise to the characteristic cytosine (C) →T and CC→TT mutations.[4]

Mutations in p53 are the most common abnormality found in human cancer. In skin tumorigenesis, mutations in p53 are the early step. The Ortonne group reported the incidence of p53 mutations to be 75%-80% in white AK patients[12]. The cells in skin epidermis lose their ability to regulate transcription of protective mechanisms, and mutant cells proliferate. Without DNA repair, cells accumulate additional mutations in tumor suppressor genes and oncogenes, which result in

over-expression of proteins and cell proliferation. Also, p53 mutations are a significant factor in the progression of precancerous AK lesions to squamous cell carcinoma.[11,4]

Inflammatory effects

The inflammatory effects of UV light absorption depend upon the particular wavelength emitted. Light of shorter wavelength has great effects on nucleic acids, amino acids, and melanin. Light of longer wavelength only affects melanin. UV light increases the metabolites of arachidonic acid, proinflammatory cytokines, adhesion molecules, and mast cell-derived mediators, leading to pro-inflammatory effects. [13]

Cyclo-oxygenase (COX) is significant for the inflammatory response before AKs develop to squamous cell carcinomas. It is the rate-limiting enzyme in the metabolism of arachidonic acid. Thus, inhibitors of COX-2, such as the non-steroidal anti-inflammatory drugs (NSAIDs) are the classical anti-inflammatory drugs in pharmacology. Based on the inflammatory mechanism, inhibition of COX-2 may be a potential therapeutic target for AK.[11]

Oxidative stress

Continual exposure of the skin to UV radiation leads to accumulation of excessive quantities of reactive oxygen species (ROS). ROS are short-lived molecular entities that are continuously generated at low levels during the course of normal aerobic metabolism. Oxidative stress represents the state of increased ROS concentration. Prolonged UV exposure releases massive amounts of ROS, causing a series of skin disorders. [14]

ROS are involved in all three tumor development stages: initiation, promotion, and progression. Thus inhibition of oxidative stress can be a potential target for the treatment of AK.[14]

1.3. Current treatment of AK

It is now clear that AK is a precursor to basal cell carcinoma and squamous cell carcinoma. However, currently there is no effective way to predict which AK lesions will evolve into invasive malignancies. Therefore, the approach to managing of AKs has been divided into lesion-directed and field-directed treatments. For lesion-directed therapy a solitary AK lesion or a small cluster of identifiable AKs are treated with cryotherapy or surgical therapy. Field directed-therapy targets the whole 'field' of visible AK lesions and AK-adjacent skin[15] using various pharmacological agents[4]. Therefore, the field-directed therapy is designed to treat multiple existing tumors as well as to inhibit the formation of new lesions in the AK-adjacent area.

1.3.1. Lesion-Directed Therapies

Cryotherapy

Cryotherapy or cryosurgery with liquid nitrogen for individual lesions is quick, low-cost and easily performed by the physician in an office-based setting. The treatment is administered by either spray or contact with the freezing liquid, destroying the epidermal keratinocytes. Where treated, the epidermis forms an ice ball. A blister then appears, indicating that the basement membrane of the lesion has been separated from the dermis. When used on thinner lesions, this technique, yields 90% clearance of AKs at 6 months[16]. However, cryotherapy may cause pain, erythema, depigmention and scarring, and it cannot be used in large skin areas[17]. There is also a long recovery period between repeat treatments.[4,7]

Surgical therapy

Surgical therapies for AKs include surgical excision, shave excision, curettage with or without electrodesiccation, and dermabrasion. None of these therapies has been evaluated in clinical trials and their use is based upon limited

evidence from small observational studies and clinical experience[18].The strong pain, unexpected infections, and widespread scarring cannot be avoided by surgical therapy. Therefore surgical therapy is not a routine treatment for AKs[4].

1.3.2. Field-Directed Therapy

5-Fluorouracil cream

Topical 5-flurourancil (5-FU) has played an important role in the treatment of AKs for decades. 5-FU is a pyrimidine analog, which halts the conversion of deoxyuradilic acid to thymidylic acid, disrupting DNA formation[19]. Through this action, 5-FU can prevent cell proliferation in AKs. 5-FU is available as a cream in 5, 1, and 0.5% concentrations, and as a solution in 5% and 2% concentrations. The 5% 5-FU cream is applied twice daily for 2-4 weeks[4]. The side effects include inflammation, erosion and ulceration during treatment. The lower concentration creams serve as an alternative treatment and result in less inflammation associated with their application. Naturally, the treatment period is prolonged because of the low drug concentration, and complete lesion clearance is poorer compared to the 5% cream. [4]

Topical diclofenac

Diclofenac is an NSAID. It inhibits the eicosanoid pathway and has high efficacy in the treatment of UVB-induced skin diseases, including AK, basal cell carcinoma and squamous cell carcinoma[4]. The most common treatment with diclofenac involves the use a 3% gel formulated with hyaluronic acid for 60-90 treatment days. The most frequent adverse effects are dry skin pruritus, erythema, and rash at the application site. Treatment with the 3% diclofenac is better tolerated than the 5-FU cream[20].

Even if field-directed therapy shows promise for complete clearance of AKs[4], this therapy unavoidably can cause morbidity in high risk individuals and

can lead to negative cosmetic outcomes. Moreover, there are safety issues associated with the currently used agents. Treatment side effects may cause interruption of treatment and use of alternative methods with lower efficacies and prolonged treatment periods. Clearly, novel agents need to be developed to achieve both high safety and efficacy for the treatment of AKs.

2. Non-melanoma Skin Cancer (NMSC)

Non-melanoma skin cancer consists of two classical types: basal cell carcinoma and squamous cell carcinoma .UV radiation is a major causative factor for NMSC. Basal cell carcinoma usually is observed as a raised, smooth pearly bump on the sun-exposed skin of the head, neck or shoulders. It grows very slowly, leading to localized skin damage. It is also the less deadly of the two, and can be easily and completely cured. Squamous cell carcinoma commonly resents as a red, scaling, thickened patch on the sun-exposed skin. Some are firm hard nodules and dome shaped. Ulceration and bleeding may occur. It is more likely to metastasize as the second most commons skin cancer. [21] There is a rough estimate: of non-melanoma skin cancers, about 80% are basal cell cancers and 20% squamous cell cancers[22].

NMSC are the most common human cancer. Even though the harmful effects of sun exposure are known to the public, its incidence continues to rise. Since 1960, a 3–8% yearly increase in the incidence of NMSC has been reported worldwide. The incidence of basal cell carcinoma is increasing by 10% worldwide, which will soon equal that of all other cancers combined. Furthermore, an estimated 40–50% of patients with a primary carcinoma will develop at least one or more basal cell carcinoma within 5 years. The estimated incidence of NMSC in the USA exceeds 1,000,000 cases per year, of which roughly 20–30% are squamous cell carcinoma.[23]

AK is a precursor of NMSC. Genetic data show that mutation of the p53 gene occurs in over 90% of squamous cell carcinoma patients[12]. Untreated AK lesions have a high risk of conversion from AK to squamous cell carcinoma[12]. In terms of a single AK, this conversion takes place at a rate of between 0.0025% and 16% per year. For multiple lesions, the annual risk of conversion is between 0.15% and 80%[2]. The existence of such a wide range in conversion rates is due to the inability to distinguish between AK lesions and squamous cell carcinoma. Although most AKs do not progress to squamous cell carcinoma, AKs that will progress to squamous cell carcinoma cannot be distinguished from those that will spontaneously resolve or persist[7]. Therefore, the treatment of AK is also a prevention approach to squamous cell carcinoma.

3. Phospho-sulindac and difluoromethylornithine: Two significant agents for skin diseases

3.1. Phospho-sulindac (PS)

NSAIDs are the most widely used anti-inflammatory compounds[24]. NSAIDs exhibit a significant anti-neoplastic effect[25] and are considered genuine anticancer agents. Sulindac is a classical NSAID. The toxicity of NSAIDs, attributed to their inhibition of COX, has limited their clinical application.

PS is a phospho-modified derivative of sulindac (Fig. 3). Structurally, PS and other phospho-NSAIDs share a common core structure: *NSAID*-*aliphatic linker*-*DEP*, where the aliphatic linker is often 1,4-butanediol, and DEP is

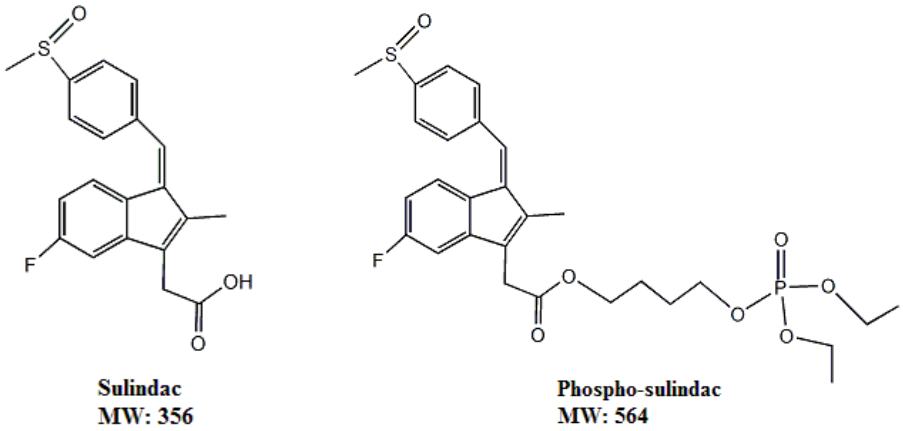

Figure 2. The structure of Sulindac and Phospho-sulindac
(Adapted from ref.**31**)

diethylphosphate[26]. Previous work has revealed that the toxicity of NSAIDs is mainly derived from their carboxylate moiety[27]. This observation provided the rationale for the chemical modification of the carboxylate group with the expectation that such modification would reduce their toxicity.

PS has shown promising chemopreventive and chemotherapeutic efficacy in preclinical models of colon, lung, and skin cancer, as well as arthritis[28,29,30]. Mechanistically, the anticancer effect of PS is mainly derived from its ability to induce ROS, and from associated effects including suppression of glutathione (GSH) levels, increased oxidized Trx-1 levels, and effects of signaling cascades, including polyamines, MAPKs and NF-κB[29]. The gastrointestinal toxicity of PS in multiple studies was essentially non-existent[29].

The major metabolites of PS are sulindac, sulindac sulphone, and sulindac sulphide[31]. In the plasma, PS is quickly hydrolyzed by carboxylesterases, which attenuate the efficacy of PS[32]. Carboxylesterases are highly expressed in the intestine, liver, and plasma[31,32]. Fortunately, the activity of carboxylesterases in the skin is 10-fold lower than in intestine, and liver [33]. Moreover, the carboxylesterase activity in humans is only 3% of that in mice[34]. Thus it is reasonable to expect that the anticancer efficacy of PS would be much higher in

humans compared to mice. Therefore, topical drug delivery is a significant approach to AK and NMSC treatment.

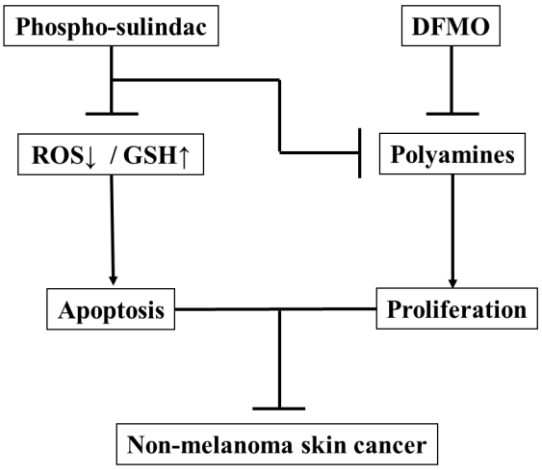

Figure 3. The effects of PS and DFMO on NMSC

3.2. D,L-α-difluoromethylornithine (DFMO)

DFMO suppresses mammalian tumor cell growth through its effect on the polyamine pathway. Polyamines are organic cations derived from amino acids, and found in every organism. Putrescine, spermidine and spermine are the main polyamines in mammalian cells[36]. The biosynthesis of polyamines is shown in Fig.5. The relationship between cell proliferation and accumulation of polyamines was reported in the 1960s[35]. In the 1980s, DFMO was designed as an ornithine decarboxylase inhibitor for the treatment of cancer[36]. ODC is the enzyme that catalyzes the first step of the synthesis of polyamines. However, DFMO by itself lacks anticancer therapeutic efficacy[36]. Currently, it holds promise for colon cancer prevention in combination with other agents, such as sulindac[37].

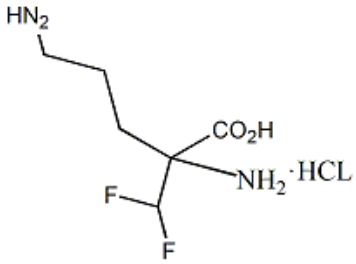

Figure 4. Structure of DFMO

Polyamines are polycationic aliphatic amines. The naturally occurring polyamines, putrescine, spermidine and spermine are widespread in nature. They have been implicated in growth and differentiation processes. Polyamines accumulate in cancerous tissues and their concentration is elevated in body fluids of cancer patients. Drugs which inhibit the synthesis of polyamines can prevent cancer and may also be used for therapeutic purposes. [38]

Inside the cell, polyamines are present at nearly millimolar concentrations. An equilibrium exists between polyamines bound to polyanionic molecules (mainly DNA and RNA) and free polyamines[39]. The free polyamine pool represents 7-10% of the total cellular polyamine content[36]. Since only the free polyamines respond immediately to cellular needs, it is not surprisingly that they are subject to strict regulation. Polyamines are maintained within very narrow range because decrease in their concentrations inhibits cell proliferation while excess appears to be toxic. [40]

Mechanistically, polyamines are involved in a large number of cellular processes. For example, polyamines participate in modulation of chromatin structure, gene transcription and translation, DNA stabilization, signal transduction, cell growth and proliferation, migration, membrane stability, functioning of ion channels and receptor-ligand interactions. [41]

Polyamine depletion induces MAPK pathway and elevates the stress-regulated kinase (JNK) activity. Increased MAPK/JNK induces p53 tumor suppressor protein, which in turn may increase the transcription of p21, inhibiting cyclin-dependent kinases and causing accumulation of the hypophosphorylated form of the retinoblastoma protein.[42]

As polyamines are tightly correlated with regulation of cellular growth, there has been an increasing effort over the past years to link polyamine metabolism to cancer. Increased polyamine levels are coupled with increased cell proliferation, decreased apoptosis and increased expression of genes associated with tumor invasion and metastasis, thus making their metabolism a target for cancer treatment and prevention. [43.36]

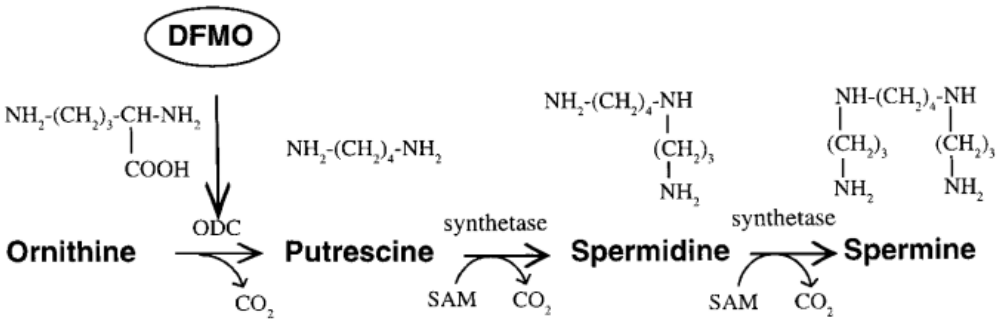

Figure 5. Effect of DFMO on the polyamine synthesis biochemical pathway
SAM: S-adenosyl methionine; ODC: ornithine decarboxylase (ref. 44)

3.3. Synergistic effect between PS and DFMO

Using drug combinations is a useful approach to overcome the limitations of NSAIDs. The combination of sulindac with DFMO is one of the most successful approaches to prevent sporadic colon adenomas[45]. DFMO inhibits ODC, which catalyzes the rate-limiting step in polyamine synthesis [46], whereas sulindac

stimulates polyamine acetylation and export[47]. The reduction on polyamines results in a suppression on cell proliferation.

Here, the synergistic effect in colon cancer between PS and DFMO was proved by Mackenzie group. The efficacy study of DFMO and PS/DFMO had significant effect on reduce putrescine and spermidine, but not spermine. PS is considered to share the same property with sulindac. The synergistic effect of PS/DFMO was reported that PS and DFMO can decrease cell proliferation by inhibition of polyamines. PS can inhibit polyamines by stimulating spermidine/spermine-N1-acetyltransferase (SAT1).[29,31,65]

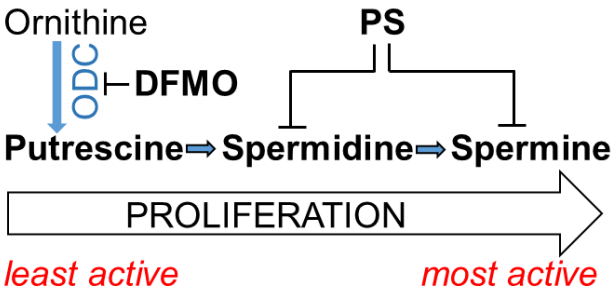

Figure 6. Synergistic effect of PS and DMFO on polyamines
(Adapted from ref. 36)

On the other hand, DFMO can affect the pharmacokinetic profile and biodistribution of PS. Our group reported pharmacokinetic studies on both PS and DFMO *in vitro* and *in vivo*. In the PS/DFMO combination, DFMO decreased the bioavailability of sulindac, sulindac sulphone and sulindac sulphide in plasma by 45%, 28% and 27% respectively, compared with PS alone. These results showed that DFMO can raise the level of intact PS in tissues[31], which may consider a method to increase PS level in tissues.

4. Topical drug application: Hydrogel vs. Organogel

As mentioned before, topical drug application, in this case transdermal drug delivery, is essential, and evidenced by a rising number of studies focusing on this area. The transdermal drug delivery system is accepted as an alternative to oral drug and injection[48]. Currently, there are 19 drugs or drug combinations administered using FDA-approved transdermal delivery systems[48]. Clinically, transdermal drug delivery is well accepted because of low-cost and self-administration. However, it is not easy to overcome the barrier of the skin, the biggest organ of the human body. An ideal formulation needs to balance penetration efficiency and safety[48].

Gel is a semi-solid material composed of low concentrations of gelator molecules that self-assemble via physical or chemical interactions into an extensive mesh network with a liquid solvent[49]. As a commonly used formulation, gel is divided into two categories based on the nature of the solvent: water in hydrogel and an organic solvent in organogel[50]. Hydrogels are prepared using natural or synthetic hydrophilic polymers, which form a colloidal network of polymer chains in water[51]. On the other hand, the use of organogel-based products is increasing due to their easy method of preparation and inherent long-term stability[51].

There have been many commercial drugs in topical formulation for AK treatment including 5-FU or diclofenac sodium hydrogels. However according to Prausnitz and Langer's classification of transdermal delivery systems[48], those commercial hydrogels belong to the first-generation delivery systems, which only allow low dose of drugs with low-molecular weight. Due to these disadvantages, the organogel has been attracting major interest. A great number of molecules are discovered or synthesized that can gel the organic solvent at a low concentration. Compared to hydrogels, gelators in organogels are normally polymers. Among organogels, lecithin organogel appears very promising.

Lecithin organogel isotropic gel composed of phospholipids (lecithin), the appropriate organic solvent, and a polar solvent[52]. Lecithin is a biocompatible surfactant as well as chemical enhancer and shows enhanced ability for skin permeation. Moreover, the amphiphilic nature of lecithin organogel allows dissolving either hydrophilic or hydrophobic drugs in the aqueous phase and organic phase, respectively[52]. The PS/DFMO drug combination benefits from this feature because PS is lipophilic and DFMO is hydrophilic.

However, lecithin organogel is limited by the requirement for high purity lecithin, which is very expensive and difficult to obtain. Recently, it is reported that synthetic polymers such as pluronics can incorporate with lecithin organogel and form a pluronic lecithin organogel (PLO)[52]. Pluronics can help lecithin organogel gel when lecithin purity is low. The term pluronics represents a series of nonionic, closely related block copolymers of ethylene oxide and propylene oxide. It is reported that in cats [53] and humans [54] PLO causes a promising enhancement of drug penetration and therapeutic effect.

5. Animal models of NMSC and AK

An animal model is an animal that is studied frequently and preferentially to tell us more about systems, tissues, cells and biochemical and physiological processes in which we are interested. In pre-clinical studies, animal models are used to predict drug efficacy and safety. Lubet's group in 2010 reported six key elements for establishing the ideal animal model for cancer: (1) the animal model has the ability to generate human cancers in a specific organ site and with a similar pathology; (2) the genetic mutation of this lesion should parallel those appearing in humans; (3) genomic changes similar to human are preferred; (4) the cancer in animal models should follow a similar process of human cancer histologically and molecularly; (5) the model should be able to produce a consistent tumor burden so that at the endpoint over 60% of animals develop the

disease; and (6) the predictive value of animal model and human efficacy data should be matched[55].

5.1. Xenograft cancer model

In the xenograft model, foreign tumors are transplanted into animals by using living cells, tissues or organs. The cancer cell line to be used in xenograft models is grown *in vitro*. The laboratory mouse with a genetic mutation, such as nude mouse and NOD/SCID mouse, is a good receptor because it cannot reject tumors or show a response to the tumor. The injection sites include subcutaneous and orthotopic sites. In our study, we used the A431 cell line as a model of epidermoid carcinoma; it can grow fast *in vivo* with a low injection volume because it massively expresses epidermal growth factor receptor, and contains no functional p53 gene[70]. One week after transdermally injecting A431 cells into NOD/SCID mice, tumors are well established. However, since these cells are grown *in vitro*, they are likely genetically different from those from which they originated[56]. Thus, such xenograft cancer models may not always generate a cancer with pathology similar to that in humans.

5.2. Chemically-induced model

The chemically-induced model of skin cancer has a long history. In the 1920s scientists noted that the carcinogenic tar generated tumors in mice. Then a two-stage protocol for chemically-induced skin cancer was developed. 7,12-dimethylbenz[a]-anthracene is a commonly used initiator which can cause gene mutations in animals. 12-O-tetradecanoylphorbol-13-acetate can maintain the gene mutation, and stimulates the formation of tumor in the second stage. Although this model has been used widely, the limitations in fundamental biology of epithelial cancer persist. Researches demonstrated that the mutated gene in

chemical-induced model is *Hras*, whereas the majority of mutations in AK and NMSC are in p53.[57]

5.3. UVB-radiation induced model

Since UVB radiation is the major cause of AK and NMSC, lesions in UVB-irradiation model have significant etiological relevance to those in humans. The tumor has been produced experimentally in animals in a way entirely similar to the production of similar tumors in human beings[58]. The popular strain of mouse used in this model is hairless albino mouse (SKh/HR1)[12]. Currently, this model develops in two stages: the *initiation stage* with single daily exposure to UVB for 10 days, and the *development stage* with only twice per week UVB exposure for 20-25 weeks[59]. With the repeated UVB irradiation, mice develop AK and squamous cell carcinoma skin lesions.

6. Assays for cell proliferation and apoptosis

6.1. PCNA as a marker of cell proliferation

Proliferating cell nuclear antigen (PCNA) plays an essential role in nucleic acid metabolism as a component of the replication and repair machinery.[60] PCNA has been shown to be an effective biomarker for cell proliferation in general and specifically in epidermal keratinocyte disorders.[61] The structure of PCNA is shown in Fig. 7.

Figure 7. Structure of human PCNA[60]

6.2. Apoptosis assay

Terminal deoxynucleotidyl transferase dUTP nick end labeling (TUNEL) is a common method for detecting DNA fragmentation that results from apoptotic signaling cascades. The principle of TUNEL is based on the presence of nicks in the DNA which can be identified by terminal deoxynucleotidyl transferase. The second label dUTPs interacts with terminal deoxynucleotidyl transferase, which indicated the DNA fragmentation. [62]

7. Biomarkers for oxidative stress

7.1. 8-hydroxy-2'-deoxyguanosine

8-hydroxy-2'-deoxyguanosine (8-OHdG), an oxidized nucleoside of DNA, is a reliable marker of DNA oxidative stress. In nuclear and mitochondrial DNA, 8-OHdG is a predominant form of free radical-induced oxidative lesions, and has therefore been widely used as a biomarker for oxidative stress and carcinogenesis. The levels of 8-OHdG can be evaluated in tissue or blood of experimental animals and humans using analytical (e.g., HPLC) and immune-histochemical methods. [63]

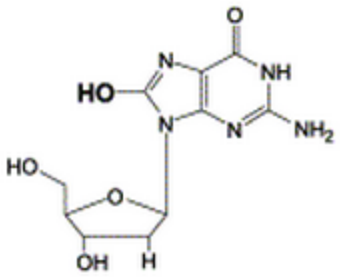

Figure 8. Structure of 8-OHdG

7.2. F2t-Isoprostane

Another biomarker of oxidative stress *in vivo* is F_{2t}-isoprostane that reflects lipid peroxidation. The oxidation of cellular lipids, typically referred to as lipid peroxidation, is a central feature of oxidant stress. F_{2t}-Isoprostane is a primary end-product of lipid peroxidation. It forms *in vivo* via a nonenzymatic mechanism involving the free radical-initiated peroxidation of arachidonic acid. F_{2t}-isoprostane is chemically stable, forms in vivo, and is measurable in all tissues and body fluids. F_{2t}-Isoprostane is a well-established tool to explore the role of oxidative stress in the pathogenesis of human diseases. Urine is always the sample of choice, since the detection of F_{2t}-Isoprostane in urine is noninvasive and this marker is not metabolized by auto-oxidation in urine. [64]

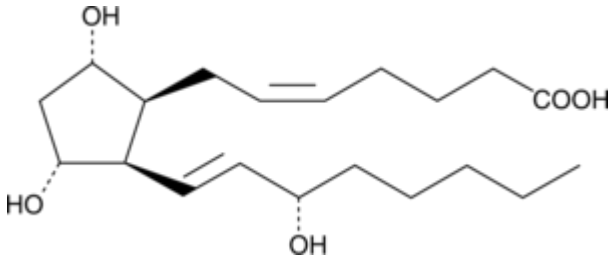

Figure 9. Structure of 15-F_{2t}-Isoprostane

8. Hypothesis

Previously published work has established the synergistic effect of PS and DFMO in the prevention of colon cancer. This was a pharmacologically documented synrgy in both cell culture systems and animals.[29]

Given the low abundance of carboxylaesterases in the skin[33], we hypothesized that the PS/DFMO combination formulated in a way that allows its topical application to the skin will be efficacious in the treatment of actinic keratosis and non-melanoma skin cancer.

To evaluate this hypothesis, we will need to ensure adequate intradermal delivery of PS and DFMO and also to assess their efficacy in appropriate animal models of these two entities. Accomplishing these goals to test our hypothesis is the subject of this thesis.

Chapter Two

Development of a Topical Treatment for NMSC and AK

1. Equipment

BRANSON 5510 Ultrasonic CleanerVortex (Branson, CT)

Centrifuge 5430 (Eppendorf, Germany)

Franz-diffusion cell (PermeGear, PA)

HPLC Waters Alliance 2695 (Waters, MA)

PowerGen Model 125 Homogenizer (Therm Fisher Scientific, MA)

Vortex-genie-2 (Scientific Industries, NY)

Water bath (Thermo Fisher Scientific, MA)

2. Mice

Female CD-1 mice aged 6 weeks at the start of the experiment were purchased from Charles River Laboratories. Animals were kept under conditions of constant temperature (23±2 ℃) and humidity (55±15%) with a 12 h light/dark cycle (lights on at 07:00 a.m), and free access to food (Purina Pico Mouse 5053) and water. All animal experiments were performed with the approval of the Institutional Animal Care and Use Committee, State University of New York at Stony Brook. Note: for the NOD/SCID, and SKH-1 mice used in the efficacy studies, we followed the same protocol.

3. Methods

3.1. Hydrogel preparation[65,66]

1 g of Pluronic P123 or F127, and estimated 70 mg of PS were dissolved into 2 ml of tetrahydrofuran. Each one of the chemical enhancers was added and mixed thoroughly by vortexing. The mixture was dialyzed for 24 hours at room temperature through a membrane (molecular weight cutoff of 3,500 Da) in PBS,

which was replaced three times. The dialysis bag was dried on the bench at room temperature until gel formation. Entrapped PS concentration was analyzed by dissolving a sample of the gel into 1ml of 100% acetonitrile. Tested chemical enhancers included lauric acid, isopropyl myristate, turpentine, azone, oleic acid and propylene glycol.

3.2. Pluronic lecithin organogel preparation[67]

PS for topical administration was formulated in a transdermal PLO gel that contained two phases: oil phase and aqueous phase.

The oil phase was prepared by mixing 3 g of lecithin and 3 g of isopropyl myristate and allowing the mixture to stand overnight at 55℃ to ensure complete dissolution. In another tube 350 mg of PS was mixed with 900 µl propylene glycol. After mixing these two parts, the chemical enhancer was added.

The aqueous phase was pluronic F127 (20%, w/w), which was prepared by adding 2 g of Pluronic F127 to 10 ml ice-cold water, placing the mixture overnight at 4℃ for complete dissolution.

The PLO gel was formed by mixing the oil phase and aqueous phases. After 3 hours, the mixture became viscous and formed a uniform gel. The resulting gel contained 3 % PS.

3.3. Harvesting of fresh mouse skin

The CD-1 mice were euthanized by CO_2 inhalation. The back part of the skin was peeled and stored at -80℃.

3.4. *In vitro* skin diffusion test

The vitro diffusion tests were carried out using the Franz diffusion cell (Fig.7) with a receptor compartment volume of 8 ml and an effective diffusion area of 1 cm^2. The Franz diffusion cell was attached to a thermostatic heater at 37±0.5 ℃

with circulating water. The receptor chamber was filled with 50% ethanol and continuously stirred with a magnetic bar at 480 rpm. The square skin sample was fixed between the receptor and donor chamber with a clamp. The system needs to equilibrate for at least 20 minutes before each experiment. The hydrogel was gently applied by a glass stick on the skin. At 0.5, 1, 2, 4, 8, 24 hours, samples were taken from the sampling port (0.3 ml) and replaced with an equal volume of fresh receptor medium. The samples were analyzed by HPLC with an excitation wavelength of 328 nm as described in a later section.

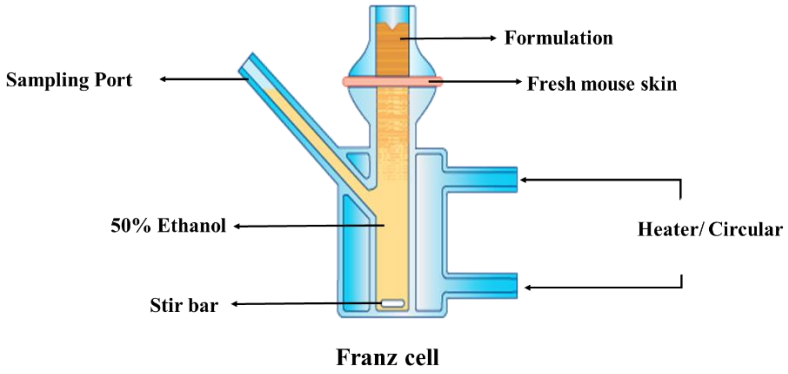

Figure 10. Franz diffusion cell

3.5. Pharmacokinetic study[31]

Female CD-1 mice were given a single dose of PS 50 mg/kg evenly applied on the whole back. Two animals were sacrificed per time point (1, 2, 4, and 6 hours). The back skin was wiped with a paper towel soaking with dd water and 10% dimethyl sulfoxide untill there was no yellow color on the paper towel (PS is yellow). The skin tissue where the drug was applied and muscle tissue beneath this site were also collected and stored in -80℃. Around 300 µl of plasma were collected by cardiac puncture. 1 ml of acetonitrile was added to plasma immediately.

The skin and muscle tissue were accurately weighted, cut and homogenized in 300 µl of dd water with the appropriate amount of 10 nM bis(4-nitrophenyl) phosphate. 1 ml of 100% acetonitrile was added into the homogenizer, and were further lysed by ultra-sonication for 15 minutes. After centrifugation at 12,000 rpm for 10 minutes, the supernatants were saved and diluted with 100 % acetonitrile. The plasma samples were centrifuged at 12,000 rpm for 10 minutes. The supernatant was saved and the level of PS and its metabolites were determined by HPLC.

3.6. HPLC analysis[31]

The HPLC system consisted of a Waters Alliance 2695 Separations Module equipped with a Waters 2998 photo-diode array detector (328 nm) (Waters, Milford, MA, USA) and a Thermo BDS Hypersil C_{18} column (150x4.6 mm, particle size 3 µm) (Thermo Fisher Scientific, Waltham, MA, USA). The mobile phase consisted of a gradient between buffer A [H_2O, acetonitrile, formic acid, 95:4.9:0.1 (v/v/v)] and 100% acetonitrile.

4. Results

4.1. Gel preparation

The amount of PS entrapped inside the pluronic hydrogel was 2.5±0.5% (w/w). The chemical enhancers were used in order to increase skin penetration. Chemical enhancers can change gel viscosity: for example oleic acid can lower gel viscosity, and isopropyl myristate can increase it (data not shown). Thus, above 15% oleic acid cannot be used in PLO formulation, because gel viscosity is too low.

The loading concentration of PS in PLO organogel was 1.5%±0.5% (w/w). DFMO was also formulated in the PLO gel. Because DFMO is water soluble, DFMO was dissolved into water before pluronic F127 was added and stirred

overnight at 4℃. The maximum concentration of DFMO in PLO gel was nearly 10.0%. Increasing the concentration of DFMO delays the time required to form a clear uniform aqueous phase.

4.2. *In vitro* skin diffusion test

The in vitro diffusion test is a method to screen chemical enhancers and uses the Franz-diffusion cell (Fig. 7). The choice of the medium in the receptor chamber is critical, since the drug needs to dissolve as quickly as possible, and the corrosion of the skin by the medium needs to be as little as possible. As a result, 50% ethanol was chosen.

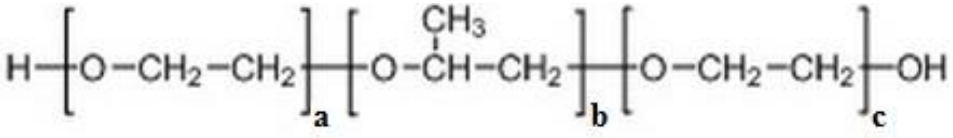

F127: a = 100 , b = 65, c = 100
P123: a = 20 , b = 70, c = 20

Figure 11. Structure of Pluronic F127 and P123
(Adapter from ref.68)

Two types of pluronic polymers P123 and F127 were used in this study. Table 1 presents the drug penetration for two pluronic-based hydrogels and the effect of chemical enhancers.

In the F127-based gel, all chemical enhancers tested increased drug permeation at 24 hours. Turpentine was the weakest enhancer and isopropyl myristate was the best. Specifically, 8% lauric acid, 5% Azone and 5% oleic acid presented approximated 10% penetration at 24 hours, whereas 15% isopropyl myristate produced 60% drug input at 24 hours, the highest level observed.

In the P123-based gel, the effect of chemical enhancers varied. Lauric acid, oleic acid, and turpentine produced a negative effect on penetration compared

with gel without enhancers. Isopropyl myristate improved the drug penetration level, but this improvement was lower than in F127-based gel.

It is clear that isopropyl myristate produced the highest permeation at 24 hours, becoming the best enhancer candidate. Enhancers in pluronic F127-based gel were better than those formulated in pluronic P123 hydrogel.

Fig. 8 shows PS penetration level in PLO gel and hydrogel. It was obvious that PLO gel even without oleic acid was better than hydrogel with 20% isopropyl myristate. However, the percentage drug input levels of the 10%, 15% and 20% oleic acid were too similar to compare.

Oleic acid and Azone in pluronic F127-based gel generated promising results. However, Azone can damage the skin during the study (also reported in the literature ref. 69). Thus, Azone data were not reported in Fig. 8. Therefore, hydrogel was ruled out, but the percentage of oleic acid is hard to determine only thought *in vitro* testing.

4.3. Pharmacokinetic study

We studied the pharmacokinetic properties of PS in mice given a single dose 50 mg/kg of PS by topical delivery (Fig. 9). Three major metabolites, sulindac, sulindac sulphide and sulindac sulphone, were detected by HPLC in plasma and skin (Fig. 10). Sulindac was the main metabolite of PS. In PLO gel with 5% oleic acid plasma C_{max} of sulindac was 9.6 μM; the T_{max} was 2 hours. In PLO gel with 10% oleic acid its plasma C_{max} of sulindac was 9.5 μM; the T_{max} was 2 hours. Emphasizing the rapid metabolic disposition of PS, plasma levels of sulindac dropped substantially at 4 h. More important, in skin tissue, PS was maintained in its intact form. In PLO gel with 5% oleic acid its plasma C_{max} of sulindac was 227.0 nmol/g; the T_{max} was 1 hour. In PLO gel with 10% oleic acid its plasma C_{max} was 208.0 nmol/g; the T_{max} was 2 hours. The PS concentration dropped dramatically after 2 h, becoming negligible at 6 h. The $AUC_{0\text{-}6h}$ of PS with PLO

plus 5% oleic acid in skin tissue from 0-6 hour was 705 nmol ħ, only slightly smaller than 746 nmol ħ in PLO with 10% oleic acid. 10% oleic acid did not show higher penetration in vivo study. Thus, for the final formulation we used PLO gel with 5% oleic acid.

5. Discussion

Topical drug treatment aims at providing high concentrations of the drug at the site of application so as to avoid adverse systemic effects associated with other routes of administration of the drug. The PLO gel was better than the previous hydrogel used in our lab, even without chemical enhancers. Oleic acid was selected as enhancer due to its safety and high penetration enhancement ability. Because there was no dialysis and evaporation step in the PLO process, this formulation can save almost 2 days compared with the previous one. PLO formulation was easily reproducible.

The pharmacokinetic study confirmed the choice of oleic acid concentration. In skin samples, the PS maintains its intact form, and only around 10% is metabolized. Sulindac, the top source of toxicity, was inhibited in transdermal delivery. This finding is in agreement with previous studies in our lab. This study demonstrated that PLO gel had the ability to raise the therapeutic effect.

Table 1. Drug penetration for two pluronic-based hydrogels with various chemical enhancers

	Pluronic			
	P123		F127	
	4h	24h	4h	24h
Enhancer (w/w)	*Drug penetration, %input*			
None	1.4	4.0	<0.6	2.3
Lauric acid				
2%	0.2	0.2	1.1	7.5
4%	1.8	0.5	0.6	9.7
8%	0.3	1.6	6.7	10.7
Isopropyl myristate				
5%	0.1	1.2	4.3	8.2
10%	1.3	5.0	2.9	9.6
15%	1.2	10.8	1.0	60.5
Turpentine				
5%	<0.1	<0.1	<1.0	<4
10%	<0.1	2.4	<1.0	<4
Azone 5%	N/A	N/A	<4.0	10.0
Oleic acid				
5%	0.3	1.6	3.9	10.6

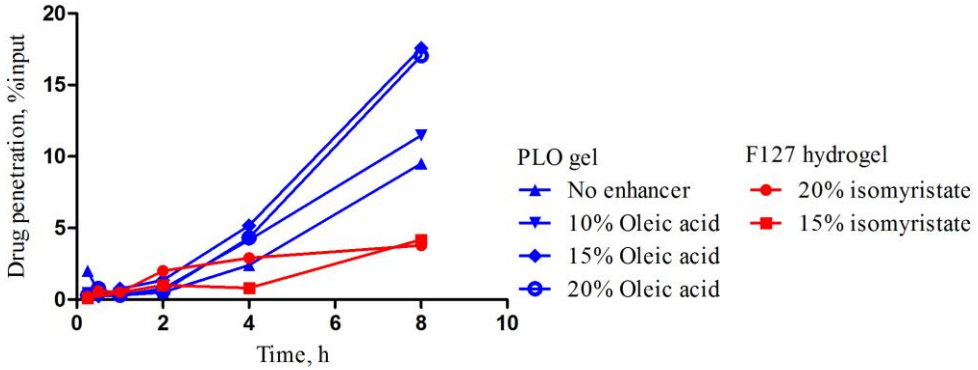

Figure 12. *In vitro* diffusion test with PLO gel and hydrogel. Various concentrations of chemical enhancers were used with PLO gel, compared with the best hydrogel-based formulations.

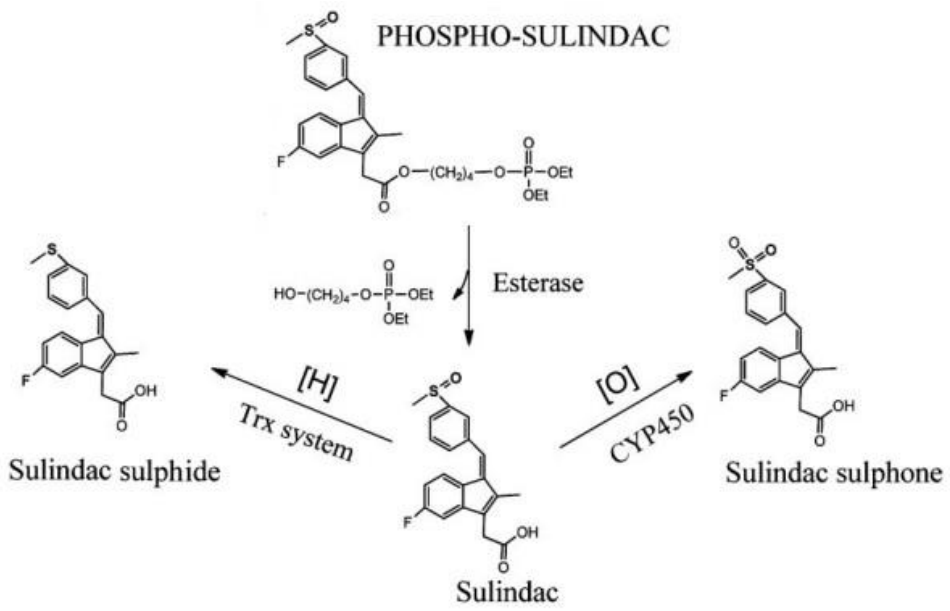

Figure 13. Pharmacokinetic study of PS (adapted from ref.31)

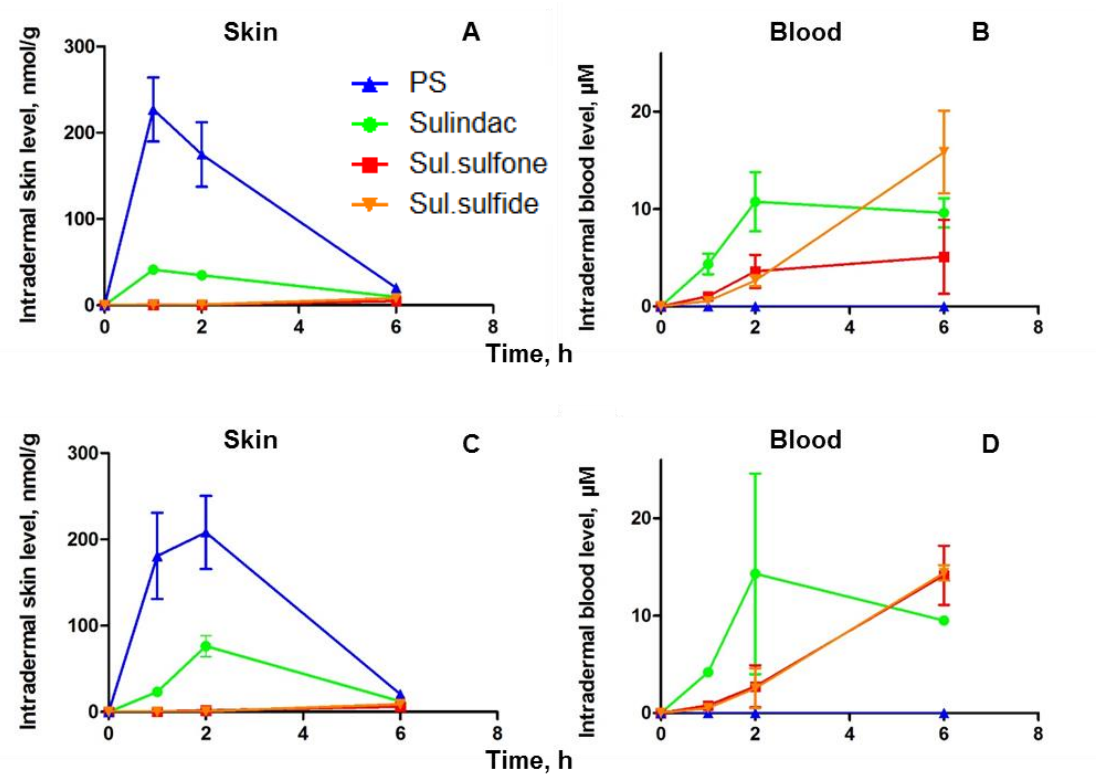

Figure 14. Typical small-scale pharmacokinetic study. PS organogel was applied to the back of mice (n=2/time point). Data are shown for PS and its metabolites determined by HPLC in skin and blood. Formulation used in A and B was1.25% PS with 5% oleic acid in PLO gel, and in the C and D was 1.25% PS with 10% oleic acid in PLO gel. Please note the scale difference (skin vs. blood).

Chapter Three

Efficacy Studies

Part I: A431 skin xenograft study

1. Method

1.1. Cell culture

The human epidermoid carcinoma cell line (A431) was obtained from American Type Culture Collection (ATCC). The cells were maintained in DMEM media (purchased from Cellgro in Herndon, VA, USA), containing 10% fetal bovine serum and penicillin/streptomycin at 37℃ with 5% CO_2. The cells were passaged 3-4 times to reach desired quantities. All experiments were performed with cells between passages 1 to 10.

1.2. Gel preparation

The methods used here are the same as in chapter two, 3.2 with the following modifications: DFMO was added as another effective component. The final aqueous phase was made by adding 1.8 g DFMO with 10 g Pluronic F127 (20%) aqueous phase, allowing the complete dissolution using a magnetic stirrer. 5% (w/w) oleic acid was added as a promising chemical enhancer into the oil phase. Blank gels were prepared by the same method but without adding PS and DFMO.

1.3. Animal model and treatment[28]

Female NOD/SCID mice were injected intradermally in both back flanks with A431 cells (2×10^6 per tumor). When the average tumor size reached 100 ± 20 mm^3, the animals were divided into four groups (i.e., 12-14 tumors/group), and were treated as follows: 1) no treatment, 2) 5% PS with 10% DFMO PLO gel (high-dose, 100 μl per treatment), 3) 1.25% PS with 2.5% DFMO PLO gel (low-

dose, 100 µl per treatment), 4) 1.25% PS with 2.5% DFMO P123 gel (pluronic hydrogel, 100 µl per treatment) twice per day, six days per week for nearly 2 weeks. The tumor size was measured twice a week with a digital microcaliper, and tumor volume was calculated using the formula: *tumor volume = [length × width (length + width/2) × 0.56]*. After treatment, the animals were euthanized and tumors were stored at -80 ℃. Body weight was recorded with every tumor size measurement.

1.4. Phospho-sulindac levels in the tumor

The tumor tissue from groups 1-4 was weighed, cut and then homogenized in 300 µl of dd water with appropriate amounts of 10nM bis(4-nitrophenyl) phosphate. 1 ml 100% acetonitrile were added to the homogenates, then tissue was further lysed by ultra-sonication for 15 minutes. After centrifugation at 12,000 rpm for 10 minutes, the supernatants were saved and diluted with 100 % acetonitrile. The PS level in the sample was detected by HPLC.

1.5. Detection of polyamines[29]

Tumor samples from groups 1-4 were accurately weighed and homogenized in fresh PBS containing 0.1 mmol/L EDTA and 1mmol/L 1,4-dithiothreitol. The homogenates were further lysed by ultra-sonication for 15 minutes. After centrifugation at 12,000 rpm for 10 minutes, the supernatants were deproteinized using 10% (v/v) perchloric acid followed by centrifugation at 12,000 rpm for 10 minutes. The samples were prepared in glass tubes: (1) skin samples: 10µl internal standard (0.5 mg/ml in 0.1N HCl) + 190 µl supernatant; (2) blank: 200 µl 0.1 M HCl; (3) polyamine standard: 10 µl internal standard (0.5 mg/ml in 0.1M HCl) + 2 µl authentic polyamine (0.5 mg/ml in 0.1N HCl) + 188 µl 0.1M HCl. To each tube we added 100 µl saturated Na_2CO_3 with 200 µl dansyl chloride (10 mg/ml in acetone). The tubes were heated at 70 ℃ for 3 hours. 20 µl of proline

(250mg/ml in water) was added to neutralize the excess dansyl chloride. The samples were incubated at 70 ℃ for 10 minutes, and cooled at room temperature. 2 ml of hexane were added, vortexed, and incubated for 5 minutes, followed by centrifugation at 1,000 rpm for 5 minutes. The supernatants were transferred to new tubes and dried. The resulting pelleted was resuspended in 1ml of 68% acetonitrile. The levels of polyamine were measured by HPLC.

1.6. HPLC analysis[33]

The HPLC system consisted of a Waters Alliance 2695 Separations Module equipped with a Waters 2998 photo-diode array detector (328 nm) (Waters, Milford, MA, USA) and a Thermo BDS Hypersil C18 column (150x4.6 mm, particle size 3 μm) (Thermo Fisher Scientific, Waltham, MA, USA). The mobile phase consisted of a gradient between buffer A [H2O, acetonitrile, formic acid, 95:4.9:0.1 (v/v/v)] and 100% acetonitrile.

2. Results

2.1. PS formulated with PLO gel inhibits the growth of A431 xenografts

We used the A431 xenograft model to evaluate the efficacy of PS/DFMO formulated in the PLO gel or hydrogel. A431 is a model cell line of epidermoid carcinoma widely used in biomedical research[70]. The NOD/SCID mice were treated with two drug concentrations in PLO gel, one drug concentration in hydrogel or control. The treatment lasted 13 days.

In the control group, the tumors grew rapidly. The tumor volume per animal was increased from 91.2 ±14.0 mm^3 to 536.1 ±29.9 mm^3. All PS/DFMO groups showed significant reduction in tumor volume compared to controls (Table 2 & Fig. 11). Numerically, the greatest reduction was obtained with PS 1.25%/DFMO

2.5%, being 70.8% (the baseline tumor volumes were factored in into these calculations).

Of note, in the hydrogel group, the tumor volume per animal remained stable until day 7. After that, the animals began to die (Fig. 12), and the survival rate dropped to 33.3% at the end of the experiment. In fact, on day 13, the number of animals in the hydrogel group was too low to be analyzable.

Interestingly, the low-dose group and high-dose PLO gel groups, the tumor volume per animal did not show any significant differences. At the end point, the tumor volume of the high dose group (257.6 ± 16.1 mm^3) was even greater than that of the lower dose group (219.4 ± 19.1 mm^3). The reason for this rather unexpected finding might be the dry skin condition in the high-dose group that may have precluded adequate drug penetration through the skin. This notion is supported by figure 14, which shows a linear relationship between tumor weight and PS levels in the tumor. Although this apparent correlation is not statistically significant (likely due to the small sample size) the observed trend suggests the dose-dependence of the therapeutic effect.

Taken together, these results indicate that PS/DFMO has a strong anticancer effect in our A431 xenograft model.

2.2. DFMO and PS/DFMO reduce the level of polyamines in human skin cancer xenografts

PS is known to reduce polyamines level in colon cancer cells. Thus, we evaluated whether PS could have a similar effect in skin cancer model. The three major polyamines molecules were examined (Fig.13). The putrescine showed the lowest level comparing to spermidine and spermine. In the treatment with 10% DFMO in high dose group, putrescine even disappeared in the tumor tissue. The two polyamines, spermidine and spermine, were reduced in the both high- and

low-dose groups, but the higher suppression was present in the low-dose group. This opposite relationship might be due to the skin rash generating in the high dose group after 8 days of treatment.

These finding indicate that PS/DFMO has a strong inhibitory effect on polyamines. Since DFMO inhibits ODC, the drug combination suppressed putrescine. However, a similar inhibition did not occur for spermidine and spermine. A biochemical explanation may lie in the fact that DFMO is a suicide inhibitor of ODC whereas PS acts through enzymatic steps that export spermine and spermidine form the cells by acetylating them.

3. Discussion

This study demonstrates that the PS/DFMO formulated with PLO gel is a strong inhibitor of NMSC in a pre-clinical model.

The PLO gel formulation improves the drug efficacy compared to the previously used hydrogel, and also yields a higher safety profile.

It is demonstrated that the polyamine pathway is one of the PS/DFMO molecular targets in NMSC, as same as it is in colon cancer[29]. The effect on polyamines also indirectly supports the notion of combining between PS and DFMO.

Regarding drug loading, the high dose group did not show the high level of efficacy that we expected. The low dose group had lesser morbidity than the high dose group. Based on the polyamines study, the low dose treatment is better than high dose from the mechanism perspective. Therefore, the preferred PS loading is 1.25%.

Table 2. Tumor volume (mm^3) in mice treated with PS/DFMO

	Day 1	Day 3	Day 7	Day 10	Day 13
Group 1 *n=6*	91.2 ±14.0	132.6 ±8.9	274.9 ± 11.3	394.7 ± 13.2	536.1 ± 29.9
Group 2 *n=7*	91.5 ±11.3	97.7 ±14.4	142.3 ± 13.7	181.8 ± 19.8	257.6 ± 16.1
Group 3 *n=6*	89.5 ±13.3	86.6 ±8.1	124.8 ± 12.3	169.5 ± 10.0	219.4 ± 19.1
Group 4 *n=6*	90.3 ±11.8	89 ±6.5	155.2 ± 17.2	223.7 ± 13.4	248.4 ± 13.4

Group 1 were control. Group 2-4 were respectively treated with 5% PS with 10% DFMO PLO gel; 1.25% PS with 2.5% DFMO PLO gel; and1.5% PS with 2.5% DFMO P123 gel. Results are presented as mean ± S.E.M.

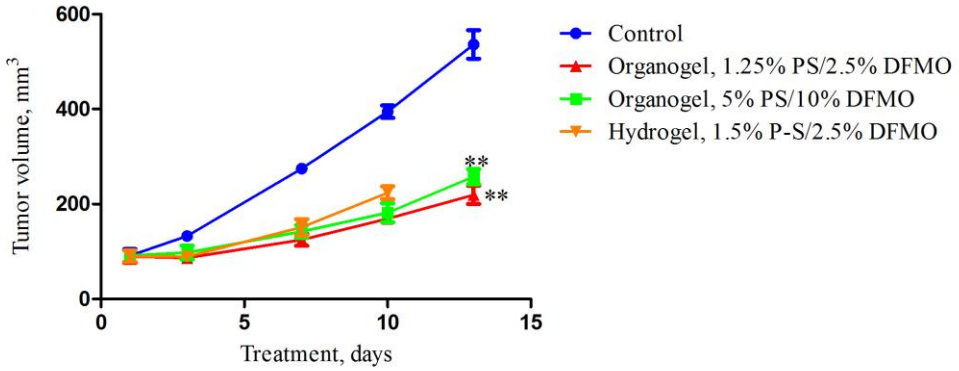

Figure 15. The effect of PS/DFMO on intradermal skin cancer
Mice were treated with PS/DFMO organogel or hydrogel as in Methods 1.3. All but two mice in the hydrogel group died on day 15, their results are not included. **: P<0.05, compared to the control group.

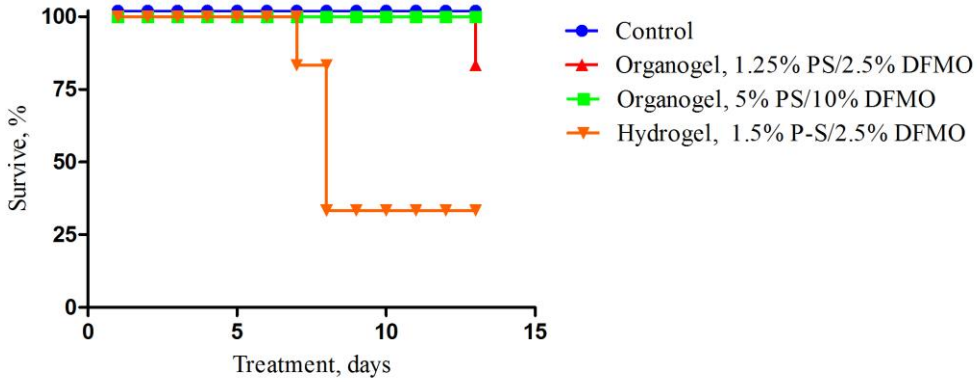

Figure 16. Survival curve of mice treated with PS/DFMO

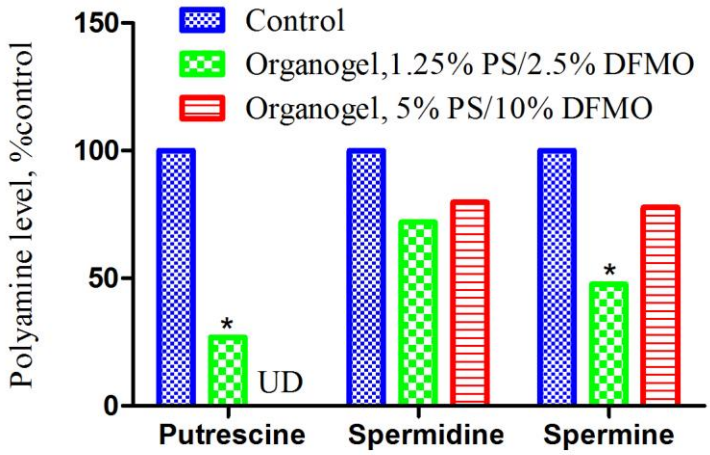

Figure 17. Polyamine levels in response to PS/DFMO *: P<0.01. Note: UD: undetected.

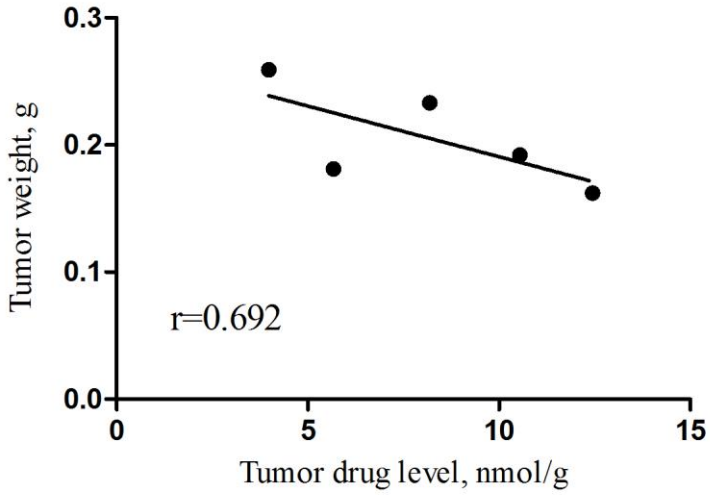

Figure 18. The relationship between tumor PS level and tumor
Mice were treated with 1.25% PS/2.5% DFMO organogel. P significant for trend.

Part II: UVB radiation–induced skin carcinogenesis study

1. Equipment

Embedding Center, Dispenser + hot Plate Leica EG1160 (Leica Biosystems, IL)

Olympus BE 41Microscope (Olympus, NY)

Richard-Allan MICROM HM 315 Rotary Microtome (Thermo Fisher Scientific, MA)

Semi-enclosed Benchtop Tissue Processor Leica TP1020 (Leica Biosystems, IL)

SpectraMax i3 microplate reader (Molecular Devices, CA)

2. Methods

2.1. Development of a UVB-radiation model[59]

The 818PH0012X6, 110-120W, 60 Hz 305-12 UVB Broadband (Daavlin, Bryan, OH) was used to produce selective broadband UVB radiation. The UVB Broadband TL lamp emits radiation in the ‘‘B’’ bandwidth of the UV spectrum (290-320 nm) and was therefore suitable for selective UVB. Light intensity was verified with the appropriate irradiation meter (Daavlin, Bryan, OH).

Seventy SKH-1 mice were divided into two groups: those receiving UV radiation, and those not exposed to it. All UVB-radiation-exposed mice were irradiated daily by UVB light with power 180 mJ/cm^2 for 75 seconds daily for a total of 10 days, representing the tumor *initiation stage*. One-week “rest” period was then implemented, when mice did not receive UVB irradiation. Following the rest period the mice were exposed with UVB light 180 mJ/cm^2 for 75 seconds twice a week for 25 weeks. This is the tumor *development stage*. When UVB radiation was terminated, each animal had 4-8 lesions. If the skin was burned or cracked, then radiation was skipped one time. Mice with large open wounds were removed from the study.

2.2. Treatment

The gel treatment began two weeks after the cessation of the UV radiation. SKH-1 hairless mice were divided into three groups. *Group1* including 12 mice was not exposed to UV radiation. *Group 2* including 24 mice was treated with 100 µl of blank PLO gel. *Group 3* including 25 mice received 100 µl of 3% PS/ 6% DFMO gel once per day. *Group 4* including 9 mice received 100 µl of 3% diclofenac PLO gel. The treatment was continued for 22 days. The gel (drug incorporated) was applied gently on the whole back between the base of the neck and the origin of the tail. Treatment of areas with visible skin damage (ulcerations, cracks) was avoided. Lesion dimensions were measured once a week with a digital microcaliper, and were calculated using the following formula: tumor volume = *[length × width × (length + width/2) × 0.56]*. The lesion number was recorded once a week. Photographs and body weight were recorded for each mouse every week.

2.3. Sample collection

On the last day of treatment, all mice including groups 1-4 were transferred to metabolic cages. After 24 hours, urine was collected, and stored at -80℃. The rest of the animals were euthanized by CO_2 inhalation. The entire back skin was collected. Half of the skin was placed in 10 % formalin for 24 hours, and the other half was cut into equal pieces and stored at -80 ℃.

2.4. Detection of polyamines

The analytical method is described in Chapter Three, part I 1.5.

2.5. Assay of urinary F_{2t}-Isoprostane

Enzymatic immunoassay for F_{2t}-urinary Isoprostane

We used the Urinary Isoprostane ELISA Kit (cat. EA85, Oxford Biomedical Research, MI). 1× wash buffer and 15-Isoprostane F_{2t} HRP conjugate (at 1:50 dilution with Enhanced Dilution Buffer) were prepared. The urine samples were thawed at room temperature. To each 100 µl urine sample we added 5 µl of glucuronidase. The tubes were sealed and votexed. The mixture was incubated at 37 ℃ for 2 hours, then diluted 1:4 with Enhanced Dilution Buffer. The standards were prepared from 1 µg/ml stock solution, and diluted as in table 3. An eight point standard curve was constructed.

Table 3. Preparation of standard curve in the urinary F_{2t}-Isoprostane assay

Standard	15-Isoprostane F_{2t} HRP concentration (ng/ml)	Enhanced dilution buffer	Transfer volume (µl)	Transfer Source
S_7	100	450	50	Standard Stock
S_6	50	200	200	S_7
S_5	10	400	100	S_6
S_4	5	200	200	S_5
S_3	1	400	100	S_4
S_2	0.1	900	100	S_3
S_1	0.05	500	500	S
B_0	0	300	---	---

100 µl of standard or diluted urine samples were added to each well on the coated plate. We made sure there was at least one duplicate for each well. 100 µl of diluted 15-Isoprostane F_{2t} HRP conjugate was added to each well omitting the reagent blank. To the reagent blanks we added 100 µl of Enhanced Dilution Buffer. The plate was incubated for 2 hours at room temperature. The washing procedure was as follows: (1) Remove the contents of each well by inversion of the plate; (2) Tap out the remaining contents of the plate onto a clean paper towel; (3) Add 300 µl of 1× wash buffer, and stand for 3 minutes; (4) Repeat procedure

two more times; (5) Remove the contents of each well by inversion of plate, and tap out the remaining contents on a clean paper towel. After three times of washing, 200 µl of TMB substrate were added to each well. The plate was incubated for 40 minutes until B_0 showed appreciable blue hue. The reaction was stopped by adding 50 µl of sulfuric acid to each well. The plate was read at 450 nm by microplate reader.

Microplate assay for creatinine

We used the Creatine Microplate Assay Kit (cat: CR01, Oxford biomedical Research, MI). Alkaline picrate reagent was prepared by adding R2 (alkali solution) to R1 (picrate solution) in a one part to five parts ratio. The standards were prepared from standard solution provided by the kit, and diluted as in table 4. The creatinine standard curve was constructed.

Table 4. Preparation of standard curve in creatinine assay

Standard	Creatinine concentration (mg/dl)	Volume of water (µl)	Volume of creatinine standard (µl)
S_1	10.0	---	110
S_2	3.0	---	110
S_3	1.0	---	110
S_4	0	110	---

Urine samples were dilute 1:4 by Enhanced Dilution Buffer. The 25 µl standards or diluted samples were added to the corresponding wells on a microplate. We made sure there was at least one duplicate for each well. 180 µl of alkaline picrate reagent was added to each well. The plate was shaken on a shaker in order to mix the solution. The plate was incubated at room temperature for 10 minutes, and read at 490 nm by microplate reader. 15 µl of R3 (acid reagent) was

added to each well. Again the plate was shaken and tapped and let stand at room temperature for 5 minutes. The plate was read at 490 nm.

2.6. Dehydration and embedding of paraffin tissue

After fixing in by 10 % formalin solution, the fixed tissues were cute into appropriate portions and placed in embedding cassettes. The tissues in the cassettes were dehydrated for paraffin embedding by a tissue processor following the set-up program: (1) 50% ethanol, 2 changes, (2) 70% ethanol, 2 changes, 1h each; (3) 80% ethanol, 2 changes, 1h each; (4) 95% ethanol, 2 changes, 1h each; (5) 100% ethanol, 3 changes, 1h each; (6) xylene or substitute (i.e. Clear Rite 3), 3 changes, 1h each; (7) paraffin wax (56-58℃), 2 changes, 1.5h each. The tissues were kept in the stand-up position in the mode, and embedded into paraffin blocks using embedding machine.

Sample tissue were cut and mounted on the microscope slices using a rotary microtome. The paraffin blocks were trimmed to an optimal cutting surface including the sample with a small paraffin frame. The blocks were cut into 5 μm slices using a brush to draw the section onto the knife holder. The slices were placed in 40-45 ℃ water bath until it expanded and its wrinkles disappeared. The flat slices were fished out by micro slices or glass slices. The slices were dried at 60℃ in the oven. Four sets of paraffin sections required for histology study, immunohistochemical staining, and TUNEL assay.

2.7. Rehydration of paraffin-embedded tissue sections

The slices were soaked in the following solutions, each for 5 minutes: (1) Xylene; (2) Xylene; (3) Xylene; (4) 100% ethanol; (5) 100% ethanol; (6) 100% ethanol; (7) 90% ethanol; (8) 70% ethanol. Tap water and dd water were used to rinse the slices.

2.8. Hematoxylin and eosin staining of paraffin sections

Paraffin sections were dewaxed and rehydrated following method chapter three, part II 2.7. The hematoxylin and eosin were filtered before use. The slices were soaked with eosin for 10 second, and immediately rinsed with dd water. Tap water was used to fix the oxidizing hematoxylin and de-staining eosin around 5-10 minutes. Slices were rinsed with dd water and dried in an oven at 60℃ overnight, and then covered with a coverslip.

2.9. Immunohistochemical study

The Histostain-Plus IHC mouse Kit (cat: 856643, Invitrogen) was used, and two types of primary antibody were PCNA mouse antibody (Cell Signaling Technology, MI) and 8-OHdG mouse antibody (Cell Signaling Technology, MI).

The immunohistochemical staining includes five main steps: rehydration, blocking, interaction with antibody, detection and chromagen. The set of paraffins section were dewaxed and rehydrated following the method described in chapter three, part II 2.7. The rehydrated slices were soaked with 0.1 M citric acid buffer (pH 6.0), and heated to boiling by microwave at power 10 for 3 minutes, then power 1 for 10 minutes in order to perform antigen retrieval. The slices were cooled down at room temperature for at least 30 minutes, and washed with dd water twice. Soaking with 3% H_2O_2 solution for 10 minutes at room temperature was used as peroxidase blocking. Again the slices were washed in dd water twice and in PBS twice for 2 minutes each. The area around the samples was dried by clean paper towel, and the sections were circled by PAP pen.

The following blocking and incubation process required a humidified and dark environment. The marked sections were incubated with serum blocking solution for 1 hour at room temperature. The first antibody was diluted on 1:1000 with the normal serum, which was recycled from the slices. The sections were incubated with the diluted first antibody overnight at 4℃. Next day, the slices were rinsed in

PBS three times for 5 minutes each. The sections were incubated with biotinylated secondary antibody for 1 hour at room temperature. Again, the slices were rinsed in PBS three times for 5 minutes each. The antigen-antibody interaction was detected by incubating the tissue sections in HRP- streptavidin solution for 1 hour at room temperature. Also, the slices were washed following the same procedure. The peroxidase substrate solution was prepare by dissolving 80 mg 3,3'-Diaminobenzidine (DAB) in 10 ml of PBS and pouring into 200 ml PBS with 40 µl of 3% H_2O_2. The color of sections were monitored by microscopy, and stopped by immersion into dd water. The slices were counterstained with hematoxylin (filtered before used) for 45 seconds. The entire set of slices was rinsed in running tap water for 1-3 minutes followed by dd water, and dried in the oven at 60℃ overnight Next day, the dried slices were covered with coverslip.

Scoring was performed as previously reported[71]. Using a light microscope at ×200 magnification, at least 5 images per animal were taken independently from high labeled to unlabeled densities. Cells with a blue nucleus were considered unlabeled, while those with a brown nucleus were considered labeled. The cell in each image was recorded and the average per slide was determined. The percentage of 8-OHdG was then calculated.

2.10. Terminal deoxynucleotidyl transferase dUTP nick end labeling (TUNEL) assay

The *In Situ* Cell Death Detection Kit, POD (cat: 11684817910, Roche) was used in this assay. The sets of paraffin sections were dewaxed and rehydrated following the method in Chapter Three, part II 2.7. The rehydrated slices were treated with proteinase K from the kit (working solution: 10-20 µg/ml in 10 mM Tris/HCl, pH 7.4-8). The slices were rinsed twice with a PBS solution. The TUNEL reaction mixture was prepared by adding total volume (50 µl) of Enzyme

Solution to 450 µl Label Solution. The area around the samples was dried by clean paper towel, and the sections were circled with a PAP pen. The whole section area was covered by adding 50 µl TUNEL reaction mixture. The slices were incubated in a humidified and dark environment for 1 hour at 37 ℃. After incubation, the slices were washed three times in PBS for 5 minutes each. The area around the sample was dried. Then 50 µl of converter-POD was added to the sample. Slices were incubated in a humidified chamber for 30 minutes at 37℃, rinsed with PBS 3 times, and soaked the slices with DAB solution (200ml PBS + 30 µl H2O2 + 80 mg DAB). The color was monitored by microscopy every 5 minutes. The slices were counterstained with hematoxylin (filtered before used) for 45 seconds. The entire set of slices was rinsed in running tap water for 1-3 minutes followed by dd water, and dried in an oven at 60℃ overnight. Next day, each of the dried slices was covered with a coverslip.

3. Results

3.1. The effect of PS/DFMO formulated with PLO on the UVB model of actinic keratosis

To evaluate the efficacy of the PS/DFMO combination in the treatment of AK, we used the UVB-radiation model. SKH-1 hairless mice were treated with vehicle, 3% PS/6% DFMO or 3% diclonfenac. At the end of the treatment period (3 weeks), the total number of skin tumors in each mouse was recorded.

The average number of lesions per mouse shows a dramatic reduction in in the PS/DFMO treatment group compared to vehicles as depicted in in Figs. 15 and 16 and summarized in Table 5.

In the vehicle group, the lesions increased progressively. The average number of lesion per mouse grew from 7.5 ±0.4 to 19.7 ±0.1, and the volume per mouse increased from 86.1 ±10.4 mm^3 to 383.9 ±49.1 mm^3. During the 22 days of

treatment, 3 out of 24 mice in this group died because of they developed significant skin ulcerations.

In the PS/DFMO group, the average number of lesion per animal was reduced from 6.4±0.5 on day 1 to 2.9±0.2 on day 22 ($p < 0.01$), and the average lesion volume per animal dropped from 79.5 ± 9.8 mm^3 on day 1 to 30.9 ±6.8 mm^3 on day 22 ($p < 0.01$). By the end of the study (day 22), compared to time 0 values, the lesion volume/mouse was 62% lower and the lesion number/mouse was 70% lower).

Compared to the vehicle group, after 1 week of treatment the tumor growth inhibition was 133.2% ($p < 0.01$); at 2 weeks it was 123.2% ($p < 0.01$) and on day 22 116.3% ($p < 0.01$).

An important parameter of AK treatment is how many animals become completely lesion free. The percentage of lesion-free mice as a result of the treatment was increasing with time and reached to 52.2% at the end of the study.

The efficacy comparison to diclofenac revealed that the effect of diclofenac gel on the growth of tumor was marginal and did not reach statistical significance. Interestingly, diclofenac had significant adverse effects. There was significant skin rash that became massive on day 7 (Fig. 19). Animals started dying because of diclofenac treatment on day 4 and by day 18, 80% of the animals were dead and the remaining 2 were euthanized because of marked weakness (Fig. 18).

3.2. Polyamine levels in PS/DFMO and vehicle groups

Fig. 20 shown the levels of skin polyamines in the various study groups. The putrescine showed the greatest reduction compared to spermidine and spermine, similar to that what was observed in xenograft model. Spermidine and spermine, were reduced 45% and 12% respectively compared to the vehicle group. This result demonstrated that in UVB-radiation model, PS/DFMO displayed the expected inhibition of molecular polyamines levels.

3.3. Oxidative stress in PS/DFMO and vehicle groups

Oxidative stress was determined using the biomarkers 8-OHdG in the skin tissue and 15-Isoprostane F_{2t} in the urine. Fig. 21 and Fig. 22 depicted our findings. Compared to the vehicle group, PS/DFMO decreased 8-OHdG in the skin by 43.4%.

Compared to no UV treated group, F_{2t}-Isoprostane in the PS/DFMO group only increased by 20%, however the F_{2t}-Isoprostane was increased in the vehicle group almost 3.5-fold. PS/DFMO returned this induction of F_{2t}-Isoprostane levels to normal.

3.4. Cell proliferation and apoptosis in PS/DFMO and vehicle groups

AK is characterized by uncontrolled cell proliferation. Cell proliferation and apoptosis in the skin tissue were determined by PCNA[72] and TUNEL[73] staining, respectively (Fig. 22).

Compared to the vehicle group, PS/DFMO decreased cell proliferation (PCNA) by 33.3%, and induced apoptosis (TUNEL) by 50% ($P<0.01$). These findings indicate that PS/DFMO profoundly suppresses proliferation and induces apoptosis in the UVB-radiation model, explaining to a first approximation the potent inhibitory effect of this drug combination.

4. Discussion

This study demonstrates that the PS/DFMO formulated in PLO gel is a strong inhibitor of AK in the UVB-radiation model. When applied topically PS/DFMO showed impressive efficacy in the treatment of AK; this effect is robust and rapid (130% reduction in lesion volume on day 7, compared to control; 51% lesion-free on day 22), and free of side effects.

The decrease of lesion volume and number as well as the progressive response of AK lesions in the PS/DFMO group is persuasive. Of interest, treatment with

diclofenac was accompanied by serious side effects that culminated in the high mortality rate.

Mechanistically, PS/DFMO has a strong cytokinetic effect: it suppresses cell proliferation and induces apoptosis. These findings provide an initial explanation of the effect of PS/DFMO in these neoplastic lesions. At a molecular level, the effect on polyamines explains in part the anti-proliferative effect. The suppression of oxidative stress may account for the pro-apoptotic effect but the exact signaling cascade(s) is not readily apparent.

Table 5. Lesion volume and lesion number in three treatment groups.

	Day1		Day 7		Day 15		Day 22	
	Volume (mm^3)	**Number**	**Volume (mm^3)**	**Number**	**Volume (mm^3)**	**Number**	**Volume (mm^3)**	**Number**
Control n=19	86.1 ± 10.4	7.5 ±0.4	207.3 ± 26.7	14.7 ±1.3	330.3 ± 40.1	17.0 ±1.5	383.9 ±49 .1	19.7 ±1.0
PS/DFMO n=25	79.5 ±9.8	6.4 ±0.5	39.3 ±5.4	7.0 ±0.5	23.0 ±3.8	4.6 ±0.3	30.9 ±6.8	2.9 ±0.2
Diclofenac n=9	311.0 ± 57.2	11.5 ±1.2	725.9 ± 273.5	10.4 ±1.0	701.0 ± 222.7	9.0 ±0	530.9 ± 130.0	9.0 ±0

Results are presented as mean ± S.E.M. Note: for the diclofenac group the last treatment day was 18.

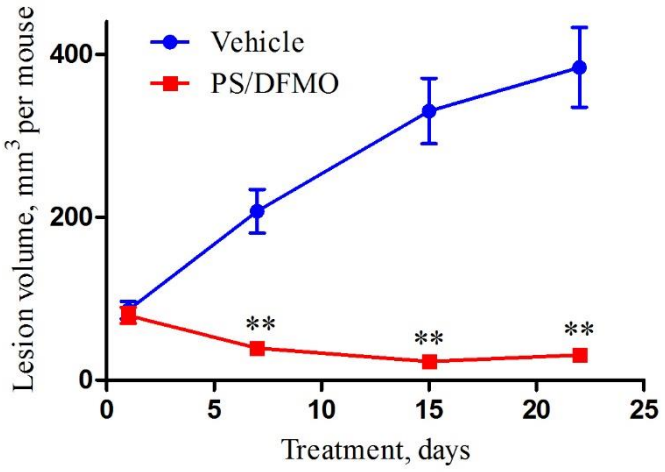

Figure 19. The effect of PS/DFMO in AK lesion volume.
**: P<0.001 compared to vehicle.

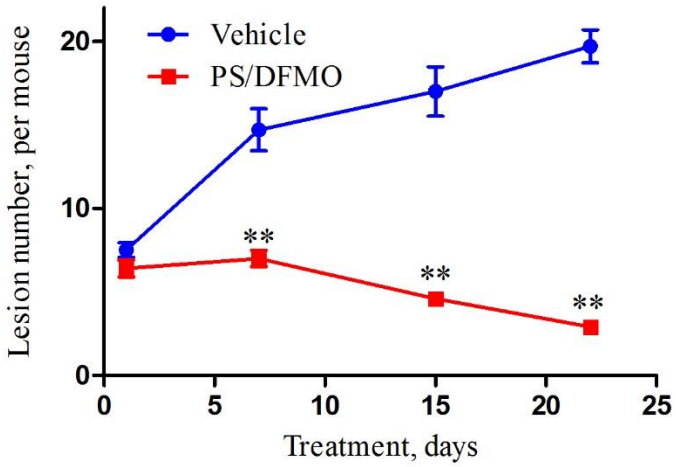

Figure 20. The effect of PS/DFMO on AK lesion number
**: P<0.001, compared to vehicle.

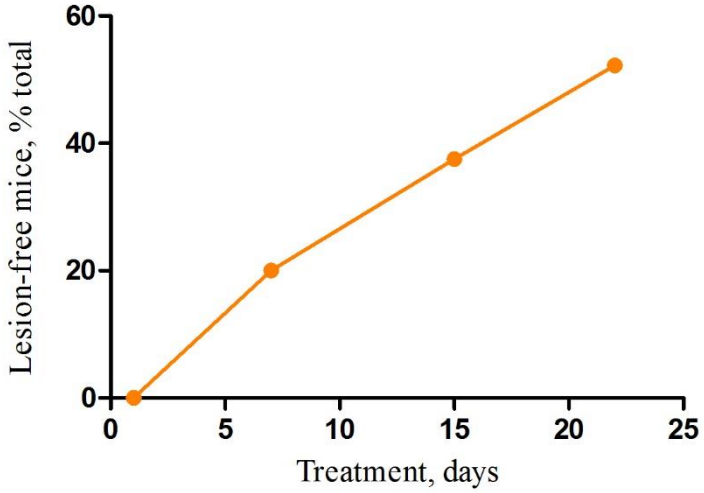

Figure 21. The number of mice that became lesion-free with PS/DFMO treatment increased with time.

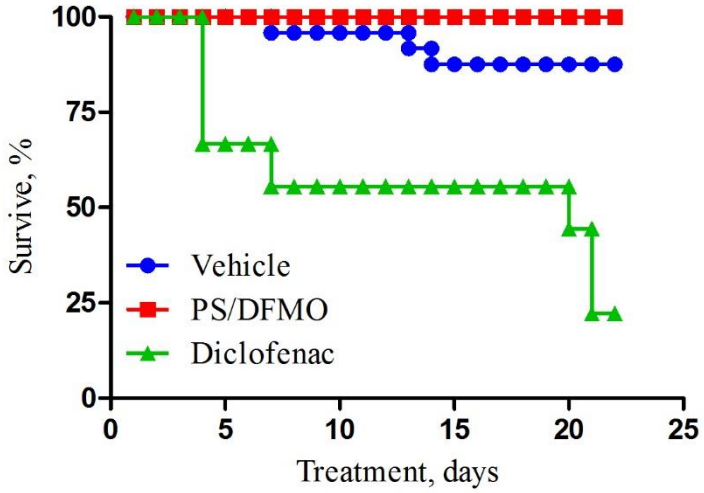

Figure 22. Survive curve for 22 day treatment period

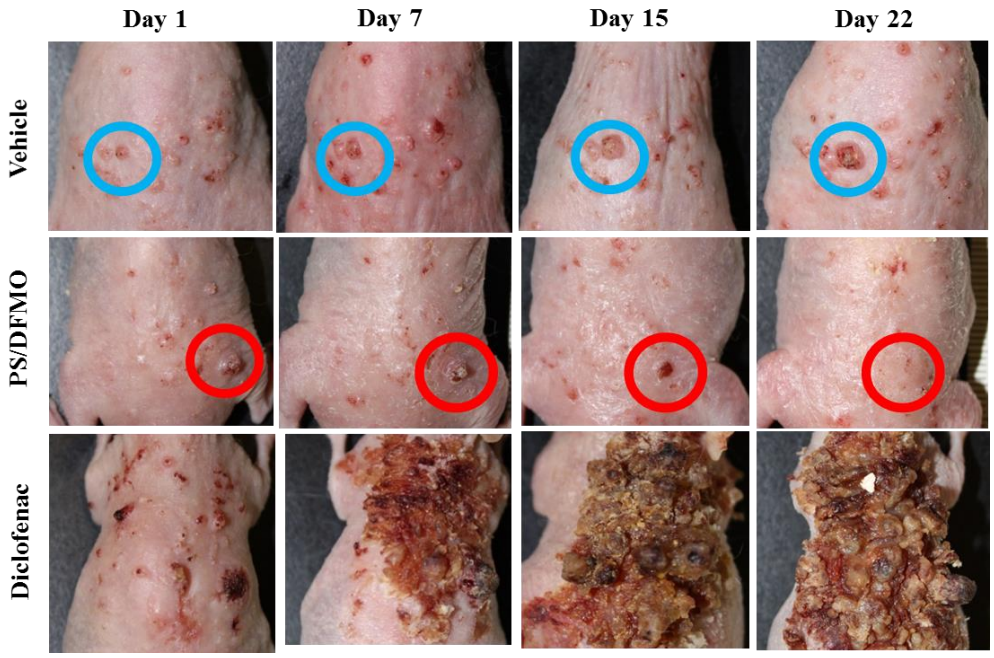

Figure 23. Progressive response of AK lesions (circled) to vehicle (top; increase), PS/DFMO (middle, decrease) during treatment. Diclofenac treatment (bottom), led to massive skin damage. The same mouse is shown in each row.

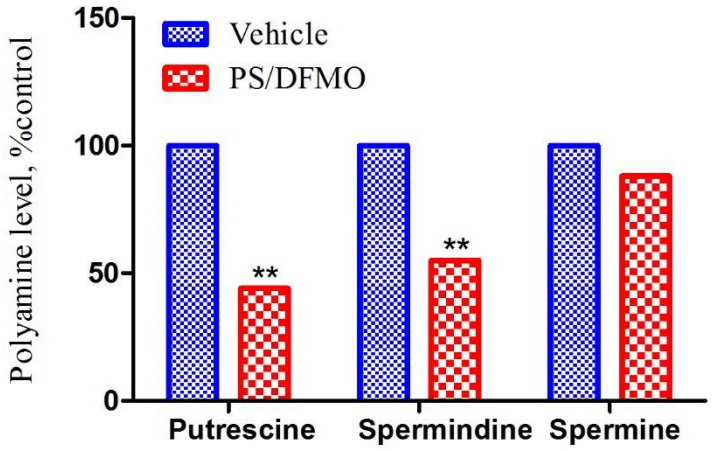

Figure 24. The polyamine levels in UVB-radiation model
**: P<0.01. Note: UD: undetected.

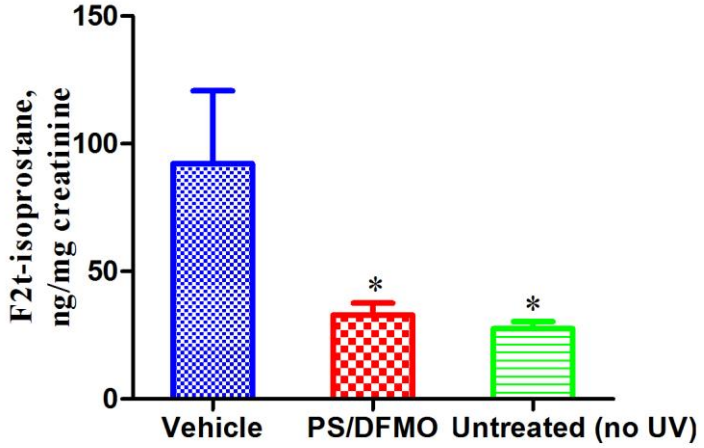

Figure 25. F2t-Isoprostane levels in the UVB-radiation model
*: P<0.05 compared to vehicle.

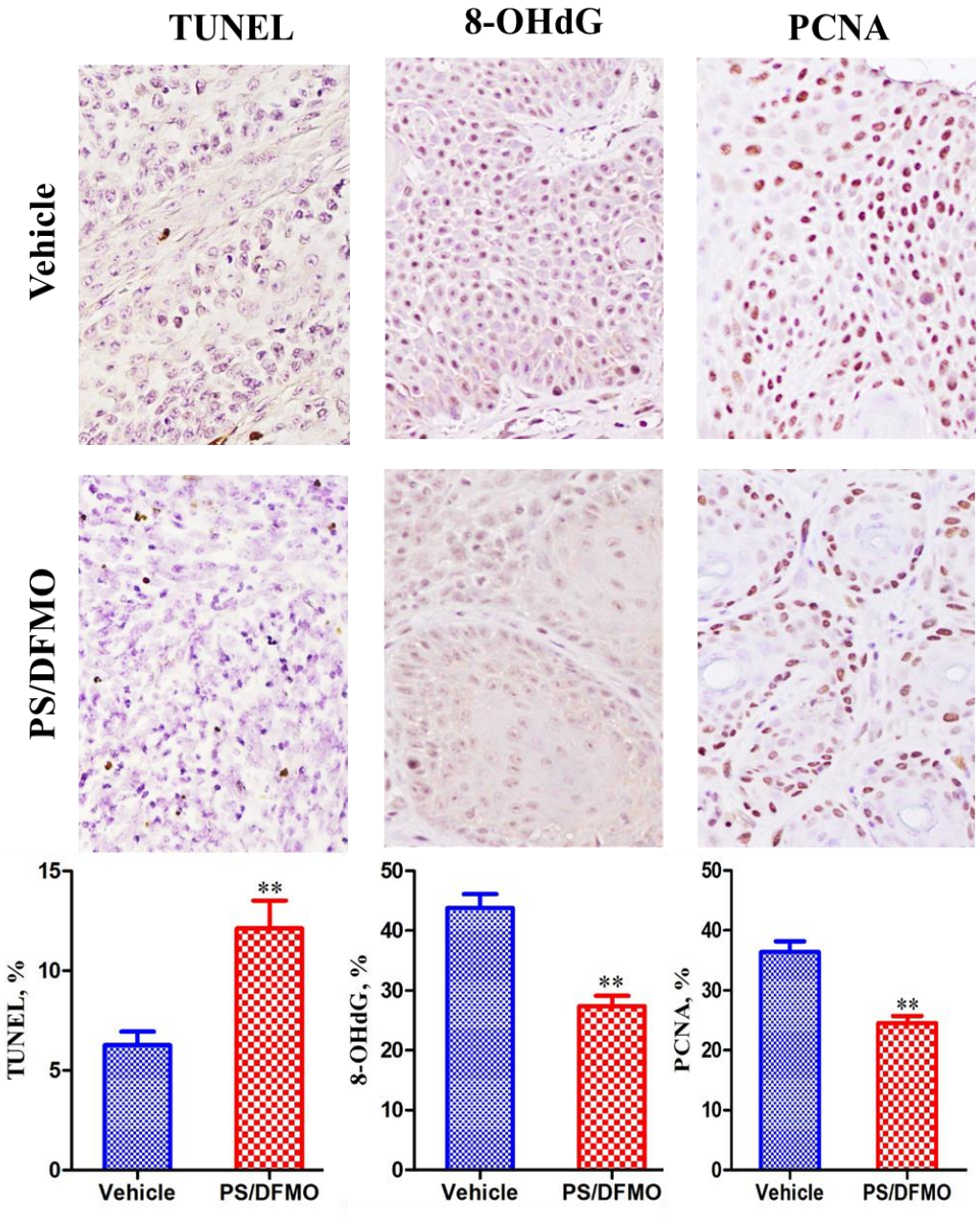

Figure 26. PS/DFMO PLO gel suppresses cell proliferation and induces apoptosis in UVB-radiation model. Left: Image of tissue stained by TUNEL method. Middle and right: Images of tissue section stained for 8-OHdG and PCNA expression. *: P<0.01 compared with vehicle.

Chapter Four
Conclusions and Future Directions

1. Conclusions and Future Directions

The symptoms and cosmetic aspects of AK are only part of its clinical importance; another part of it stems from the high prevalence of AK and its ability to progress to skin cancer. AK affects up to one in four adults and its incidence increases with age reaching 68%-79% in those aged 60-69 years. Strong evidence supports the concept that AK should no longer be considered premalignant. The importance of NMSC is also significant and based on its huge prevalence and clinical behavior.

The efficacy of current therapies for AK is suboptimal. As mentioned, these therapies have major limitations: prolonged treatment requiring weeks of application; often limited efficacy; high rates of recurrence (up to 70%); and high frequency of side effects. In fact, patient adherence to topical therapies is suboptimal or low, due to the long duration of treatment and the high frequency of adverse events. Our approach presented here aimed at overcoming these limitations.

The topical treatment of both these partially overlapping entities with the combination of PS and DFMO formulated in an organogel appears very promising. In addition to offering the advantages of topical drug delivery, PS/DFMO showed strong efficacy and no detectable side effects. Thus it is conceivable that PS/DFMO will have a major impact on the treatment of AK and NMSC because it could be superior to the currently available approaches in terms of efficacy, safety, short duration of treatment, and low cost.

We have obtained only the broad outlines of this encouraging result. Polyamines and oxidative stress seem to be important players, but it would be

unlikely to be the only drivers of the mechanism of action of PS/DFMO. Indeed, this will be an area of future study. In addition to their inherent value, mechanistic studies may help further enhance the efficacy of this combination.

Another area of future work is the further optimization of the formulation of this drug combination. Nonetheless, our findings are encouraging and it seems not unlikely that this potential product could find its way towards clinical evaluation.

References

1 Trakatelli, Myrto, et al. "Epidemiology of nonmelanoma skin cancer (NMSC) in Europe: accurate and comparable data are needed for effective public health monitoring and interventions." *British journal of dermatology* 156.s3 (2007): 1-7.

2 Ratushny, Vladimir, et al. "From keratinocyte to cancer: the pathogenesis and modeling of cutaneous squamous cell carcinoma." *The Journal of clinical investigation* 122.122 (2) (2012): 464-472.

3 Moy, Ronald L. "Clinical presentation of actinic keratoses and squamous cell carcinoma." *Journal of the American Academy of Dermatology* 42.1 (2000): S8-S10.

4 Dodds, Annabel, Alvin Chia, and Stephen Shumack. "Actinic keratosis: rationale and management." Dermatology and therapy 4, no. 1 (2014): 11-31.

5 Jackson, Sarah, Catherine Harwood, Miranda Thomas, Lawrence Banks, and Alan Storey. "Role of Bak in UV-induced apoptosis in skin cancer and abrogation by HPV E6 proteins." Genes & development 14, no. 23 (2000): 3065-3073.

6 Rosen, Theodore, and Mark G. Lebwohl. "Prevalence and awareness of actinic keratosis: barriers and opportunities." Journal of the American Academy of Dermatology 68, no. 1 (2013): S2-S9.

7 reprint from UpToDate, Official, Joseph Jorizzo, Robert P. Dellavalle, June K. Robinson, and Rosamaria Corona. "Treatment of actinic keratosis."

8 Halpern, Allan C., and Laura J. Hanson. "Awareness of, knowledge of and attitudes to nonmelanoma skin cancer (NMSC) and actinic keratosis (AK) among physicians." International journal of dermatology 43, no. 9 (2004): 638-642.

9 Alam, Murad, Leonard H. Goldberg, Sirunya Silapunt, Erin S. Gardner, Sara S. Strom, Alfred W. Rademaker, and David J. Margolis. "Delayed treatment and continued growth of nonmelanoma skin cancer." Journal of the American Academy of Dermatology 64, no. 5 (2011): 839-848.

10 Timares, Laura, Santosh K. Katiyar, and Craig A. Elmets. "DNA Damage, Apoptosis and Langerhans Cells—Activators of UV-induced Immune Tolerance†." Photochemistry and photobiology 84, no. 2 (2008): 422-436.

11 Berman, Brian, and Clay J. Cockerell. "Pathobiology of actinic keratosis: ultraviolet-dependent keratinocyte proliferation." Journal of the American Academy of Dermatology 68, no. 1 (2013): S10-S19.

12 Ortonne, J-P. "From actinic keratosis to squamous cell carcinoma." British Journal of Dermatology 146, no. s61 (2002): 20-23.

13 Wang, Lena, William Eng, and Clay J. Cockerell. "Effects of ultraviolet irradiation on inflammation in the skin." Advances in dermatology 18 (2001): 247-286.

14 Bickers, David R., and Mohammad Athar. "Oxidative stress in the pathogenesis of skin disease." Journal of Investigative Dermatology 126.12 (2006): 2565-2575.
15 Slaughter, Danely P., Harry W. Southwick, and Walter Smejkal. "“Field cancerization” in oral stratified squamous epithelium. Clinical implications of multicentric origin." Cancer 6, no. 5 (1953): 963-968.
16 Kaufmann, R., L. Spelman, W. Weightman, J. Reifenberger, R-M. Szeimies, E. V. E. L. I. E. N. Verhaeghe, N. Kerrouche, V. Sorba, H. Villemagne, and L. E. Rhodes. "Multicentre intraindividual randomized trial of topical methyl aminolaevulinate–photodynamic therapy vs. cryotherapy for multiple actinic keratoses on the extremities." British Journal of Dermatology 158, no. 5 (2008): 994-999.
17 Hantash, Basil M., Daniel B. Stewart, Zachary A. Cooper, Wingfield E. Rehmus, R. James Koch, and Susan M. Swetter. "Facial resurfacing for nonmelanoma skin cancer prophylaxis." Archives of dermatology 142, no. 8 (2006): 976-982.
18 COLEMAN, WILLIAM P., John M. Yarborough, and Stephen H. Mandy. "Dermabrasion for prophylaxis and treatment of actinic keratoses."Dermatologic surgery 22, no. 1 (1996): 17-21.
19 Eaglstein, William H., Gerald D. Weinstein, and Phillip Frost. "Fluorouracil: mechanism of action in human skin and actinic keratoses: I. Effect on DNA synthesis in vivo." Archives of dermatology 101, no. 2 (1970): 132-139.
20 Gebauer, Kurt, Pam Brown, and George Varigos. "Topical diclofenac in hyaluronan gel for the treatment of solar keratoses." Australasian journal of dermatology 44, no. 1 (2003): 40-43.
21 Cakir, Burak Ömür, Peter Adamson, and Cemal Cingi. "Epidemiology and economic burden of nonmelanoma skin cancer." Facial plastic surgery clinics of North America 20, no. 4 (2012): 419-422.
22 Marsden, edited by Sajjad Rajpar, Jerry (2008). ABC of skin cancer. Malden, Mass.: Blackwell Pub. pp. 5–6.
23 Madan, Vishal, John T. Lear, and Rolf-Markus Szeimies. "Non-melanoma skin cancer." The Lancet 375.9715 (2010): 673-685.
24 Wallace, John L. "Nonsteroidal anti-inflammatory drugs and gastroenteropathy: the second hundred years." Gastroenterology 112, no. 3 (1997): 1000-1016.
25 Grivennikov, Sergei I., Florian R. Greten, and Michael Karin. "Immunity, inflammation, and cancer." Cell 140, no. 6 (2010): 883-899.
26 Huang, Liqun, Gerardo G. Mackenzie, Yu Sun, Nengtai Ouyang, Gang Xie, Kvetoslava Vrankova, Despina Komninou, and Basil Rigas. "Chemotherapeutic

properties of phospho-nonsteroidal anti-inflammatory drugs, a new class of anticancer compounds." Cancer research 71, no. 24 (2011): 7617-7627.
27 Piazza, Gary A., Adam B. Keeton, Heather N. Tinsley, Bernard D. Gary, Jason D. Whitt, Bini Mathew, Jose Thaiparambil et al. "A novel sulindac derivative that does not inhibit cyclooxygenases but potently inhibits colon tumor cell growth and induces apoptosis with antitumor activity." Cancer Prevention Research 2, no. 6 (2009): 572-580.
28 Cheng, Ka Wing, George Mattheolabakis, Chi C. Wong, Nengtai Ouyang, Liqun Huang, Panayiotis P. Constantinides, and Basil Rigas. "Topical phospho-sulindac (OXT-328) is effective in the treatment of non-melanoma skin cancer."International journal of oncology 41, no. 4 (2012): 1199-1203.
29 Mackenzie, Gerardo G., Yu Sun, Liqun Huang, Gang Xie, Nengtai Ouyang, Ramesh C. Gupta, Francis Johnson, Despina Komninou, Levy Kopelovich, and Basil Rigas. "Phospho-sulindac (OXT-328), a novel sulindac derivative, is safe and effective in colon cancer prevention in mice." Gastroenterology 139, no. 4 (2010): 1320-1332.
30 Zhu, Rongrong, Ka-Wing Cheng, Gerardo Mackenzie, Liqun Huang, Yu Sun, Gang Xie, Kveta Vrankova, Panayiotis P. Constantinides, and Basil Rigas. "Phospho-sulindac (OXT-328) inhibits the growth of human lung cancer xenografts in mice: enhanced efficacy and mitochondria targeting by its formulation in solid lipid nanoparticles." Pharmaceutical research 29, no. 11 (2012): 3090-3101.
31 Xie, G., T. Nie, G. G. Mackenzie, Y. Sun, L. Huang, N. Ouyang, N. Alston et al. "The metabolism and pharmacokinetics of phospho-sulindac (OXT-328) and the effect of difluoromethylornithine." British journal of pharmacology 165, no. 7 (2012): 2152-2166.
32 Wong, Chi C., Ka-Wing Cheng, Gang Xie, Dingying Zhou, Cai-Hua Zhu, Panayiotis P. Constantinides, and Basil Rigas. "Carboxylesterases 1 and 2 hydrolyze phospho-nonsteroidal anti-inflammatory drugs: relevance to their pharmacological activity." Journal of Pharmacology and Experimental Therapeutics 340, no. 2 (2012): 422-432.
33 Ahmed, Shamim, Teruko Imai, Yasushi Yoshigae, and Masaki Otagiri. "Stereospecific activity and nature of metabolizing esterases for propranolol prodrug in hairless mouse skin, liver and plasma." Life sciences 61, no. 19 (1997): 1879-1887.
34 Rudakova, E. V., N. P. Boltneva, and G. F. Makhaeva. "Comparative analysis of esterase activities of human, mouse, and rat blood." Bulletin of experimental biology and medicine 152, no. 1 (2011): 73-75.

35 Russell, Diane, and Solomon H. Snyder. "Amine synthesis in rapidly growing tissues: ornithine decarboxylase activity in regenerating rat liver, chick embryo, and various tumors." Proceedings of the National Academy of Sciences of the United States of America 60.4 (1968): 1420.
36 Gerner, Eugene W., and Frank L. Meyskens. "Polyamines and cancer: old molecules, new understanding." Nature Reviews Cancer 4.10 (2004): 781-792.
37 Meyskens, Frank L., et al. "Difluoromethylornithine plus sulindac for the prevention of sporadic colorectal adenomas: a randomized placebo-controlled, double-blind trial." Cancer Prevention Research 1.1 (2008): 32-38.
38 Bachrach, U. "Polyamines and cancer: minireview article." Amino acids 26.4 (2004): 307-309.
39 Igarashi, Kazuei, and Keiko Kashiwagi. "Polyamines: mysterious modulators of cellular functions." Biochemical and biophysical research communications271.3 (2000): 559-564.
40 Minois, Nadège, Didac Carmona-Gutierrez, and Frank Madeo. "Polyamines in aging and disease." Aging (Albany NY) 3.8 (2011): 716.
41 Landau, Guy, et al. "The role of polyamines in supporting growth of mammalian cells is mediated through their requirement for translation initiation and elongation." Journal of Biological Chemistry 285.17 (2010): 12474-12481.
42 Zou, Tongtong, et al. "Polyamines modulate the subcellular localization of RNA-binding protein HuR through AMP-activated protein kinase-regulated phosphorylation and acetylation of importin alpha1." Biochem. J 409 (2008): 389-398.
43 Xie, Xiaozhen, Margaret E. Tome, and Eugene W. Gerner. "Loss of intracellular putrescine pool-size regulation induces apoptosis." Experimental cell research 230.2 (1997): 386-392.
44 Alberts, David S., et al. "Chemoprevention of human actinic keratoses by topical 2-(difluoromethyl)-dl-ornithine." Cancer Epidemiology Biomarkers & Prevention 9.12 (2000): 1281-1286.
45 Meyskens, Frank L., et al. "Difluoromethylornithine plus sulindac for the prevention of sporadic colorectal adenomas: a randomized placebo-controlled, double-blind trial." Cancer Prevention Research 1.1 (2008): 32-38.
46 Qu, Ning, et al. "Inhibition of human ornithine decarboxylase activity by enantiomers of difluoromethylornithine." Biochem. J 375 (2003): 465-470.
47 Piazza, Gary A., et al. "A novel sulindac derivative that does not inhibit cyclooxygenases but potently inhibits colon tumor cell growth and induces apoptosis with antitumor activity." Cancer Prevention Research 2.6 (2009): 572-580.

48 Prausnitz, Mark R., and Robert Langer. "Transdermal drug delivery." Nature biotechnology 26.11 (2008): 1261-1268.
49 Li, Jing Liang, and Xiang Yang Liu, eds. Soft Fibrillar Materials: Fabrication and Applications. John Wiley & Sons, 2013.
50 Vintiloiu, Anda, and Jean-Christophe Leroux. "Organogels and their use in drug delivery—a review." Journal of Controlled Release 125.3 (2008): 179-192.
51 Ibrahim, Mahmoud Mokhtar, Salma A. Hafez, and Mahmoud M. Mahdy. "Organogels, hydrogels and bigels as transdermal delivery systems for diltiazem hydrochloride." Asian Journal of Pharmaceutical Sciences 8.1 (2013): 48-57.
52 Kumar, Rajiv, and Om Prakash Katare. "Lecithin organogels as a potential phospholipid-structured system for topical drug delivery: a review." AAPS pharmscitech 6.2 (2005): E298-E310.
53 Ciribassi, John, et al. "Comparative bioavailability of fluoxetine after transdermal and oral administration to healthy cats." American journal of veterinary research 64.8 (2003): 994-998.
54 Giordano, James, Charles Daleo, and Steven M. Sacks. "Topical ondansetron attenuates nociceptive and inflammatory effects of intradermal capsaicin in humans." European journal of pharmacology 354.1 (1998): R13-R14.
55 Steele, Vernon E., and Ronald A. Lubet. "The use of animal models for cancer chemoprevention drug development." Seminars in oncology. Vol. 37. No. 4. WB Saunders, 2010.
56 Kortenhorst, Madeleine SQ, et al. "Analysis of the genomic response of human prostate cancer cells to histone deacetylase inhibitors." Epigenetics 8.9 (2013): 907-920.
57 Abel, Erika L., et al. "Multi-stage chemical carcinogenesis in mouse skin: fundamentals and applications." Nature protocols 4.9 (2009): 1350-1362.
58 Winkelmann, R. K., Edward J. Baldes, and Paul E. Zollman. "Squamous Cell Tumors Induced in Hairless Mice with Ultraviolet Light1." Journal of investigative dermatology 34.2 (1960): 131-138.
59 Phillips, Jeffrey, et al. "Curcumin Inhibits UV Radiation–Induced Skin Cancer in SKH-1 Mice." Otolaryngology--Head and Neck Surgery (2013): 0194599813476845.
60 Kelman, Zvi. "PCNA: structure, functions and interactions." Oncogene 14.6 (1997): 629-640.
61 Kanitakis, J., et al. "Keratinocyte proliferation in epidermal keratinocyte disorders evaluated through PCNA/cyclin immunolabelling and AgNOR counting." Acta dermato-venereologica 73.5 (1993): 370-375.

62 Gavrieli, Yael, Yoav Sherman, and Shmuel A. Ben-Sasson. "Identification of programmed cell death in situ via specific labeling of nuclear DNA fragmentation." The Journal of cell biology 119.3 (1992): 493-501.
63 Wu, Lily L., et al. "Urinary 8-OHdG: a marker of oxidative stress to DNA and a risk factor for cancer, atherosclerosis and diabetics." Clinica Chimica Acta339.1 (2004): 1-9.
64 Milne, Ginger L., Erik S. Musiek, and Jason D. Morrow. "F2-isoprostanes as markers of oxidative stress in vivo: an overview." Biomarkers 10.S1 (2005): 10-23.
65 Cheng, Ka Wing, et al. "Topical phospho-sulindac (OXT-328) is effective in the treatment of non-melanoma skin cancer." International journal of oncology 41.4 (2012): 1199-1203.
66 Mattheolabakis, George, et al. "Topically applied phospho-sulindac hydrogel is efficacious and safe in the treatment of experimental arthritis in rats."Pharmaceutical research 30.6 (2013): 1471-1482.
67 Murdan, Sudaxshina. "A review of pluronic lecithin organogel as a topical and transdermal drug delivery system." Hospital pharmacist 12.7 (2005): 267-270.
68 Zhang, Wei, et al. "Multifunctional Pluronic P123/F127 mixed polymeric micelles loaded with paclitaxel for the treatment of multidrug resistant tumors."Biomaterials 32.11 (2011): 2894-2906.
69 Barry, Brian W. "Mode of action of penetration enhancers in human skin."Journal of Controlled Release 6.1 (1987): 85-97.
70 A431 - Cytokines and Cells Online Pathfinder Encyclopaedia.
71 Kozoni, Vassiliki, et al. "The effect of lithocholic acid on proliferation and apoptosis during the early stages of colon carcinogenesis: differential effect on apoptosis in the presence of a colon carcinogen." Carcinogenesis 21.5 (2000): 999-1005.
72 Cozzi, Sarah-Jane, et al. "Ingenol mebutate field-directed treatment of UVB-damaged skin reduces lesion formation and removes mutant p53 patches."Journal of Investigative Dermatology 132.4 (2012): 1263-1271.
73 Gavrieli, Yael, Yoav Sherman, and Shmuel A. Ben-Sasson. "Identification of programmed cell death in situ via specific labeling of nuclear DNA fragmentation." The Journal of cell biology 119.3 (1992): 493-501.